Diffusion of electric vehicles and their flexibility potential for smoothing residual demand - A spatio-temporal analysis for Germany

AUTHORS

Fabian Arnold

Arne Lilienkamp

Nils Namockel

EWI Working Paper, No 23/04

May 2023

Institute of Energy Economics at the University of Cologne (EWI)
www.ewi.uni-koeln.de

Institute of Energy Economics
at the University of Cologne (EWI)

Alte Wagenfabrik
Vogelsanger Str. 321a
50827 Köln
Germany

Tel.: +49 (0)221 277 29-100
Fax: +49 (0)221 277 29-400
www.ewi.uni-koeln.de

CORRESPONDING AUTHOR

Fabian Arnold
Fabian.arnold@ewi.uni-koeln.de

ISSN: 1862-3808

Diffusion of electric vehicles and their flexibility potential for smoothing residual demand - A spatio-temporal analysis for Germany

Fabian Arnold[a,*], Arne Lilienkamp[a], Nils Namockel[a]

[a] *Institute of Energy Economics at the University of Cologne, Vogelsanger Strasse 321a, 50827 Cologne, Germany.*

Abstract

The transformation of the energy system causes increasing stress on distribution grid components. However, flexible EV charging, if incentivized adequately, can help mitigate this impact by reducing peaks in loads and feed-in. A comprehensive regional analysis is necessary to understand the potential of EV charging flexibility for reducing peaks on regional and national levels. To this end, we estimate regional residual demand time series for Germany for the years 2019, 2030 and 2045. We focus on modelling private EV diffusion via sigmoid functions and deriving driving and charging profiles based on micro mobility data. Further, we distinguish two deployment schemes for EV flexibility: (1) all EVs contribute to flattening the national residual load curve; (2) local EVs contribute to flattening regional residual load curves. We find that the residual load curves change structurally as positive and negative peaks in residual demand increase over the years on the regional and national levels. Although the absolute flexibility potential of EV home charging increases with the number of vehicles, its marginal utility to reduce load peaks declines.

Especially in load-dominated regions, the national deployment of flexibility can result in higher regional demand peaks compared to a scenario without charging flexibility. The two approaches of flexibility activation can be contradictory in their effects: While regional incentivization is less efficient in reaching the smoothing in the national residual demand curve, national incentivization can even lead to increased strain on the local level.

Keywords: Flexibility, Electric vehicles, Residual load, Energy transition, Charging profiles

JEL classification: C61, D47, O33, Q41, Q48

The contents of this paper reflect the opinions of its authors only and not those of EWI.

*Corresponding author, *email*: fabian.arnold@ewi.uni-koeln.de. The authors are listed alphabetically by last name and contributed equally to this paper.

1. Introduction

The energy transition towards a decarbonized future brings about fundamental changes in the established power system, including increasing strain on distribution grid components. First, the widespread implementation of decentralized renewable energy systems, such as wind and photovoltaic (PV) systems, which are mostly connected to the low and medium-voltage grid, increases the feed-in of electricity into the distribution grid. Second, new demand applications emerge in the distribution grid, e.g., charging electric vehicles (EV), increasing the load. Both developments increase load and feed-in peaks on the national level as well as place an additional burden on the technical components of local grids, such as low and medium-voltage transformers, which were designed under different conditions and may need to be replaced or expanded to accommodate the changes. The charging of EVs can increase peak load and put a strain on existing distribution grid equipment. However, the flexibility in EV charging offers a solution to mitigate this impact. By charging during periods of high renewable energy generation, load and feed-in peaks can be reduced, thus reducing the strain on the grid.

The availability and necessity of EV charging flexibility depend on various regionally distinct factors, such as the share of the EV load in the total load, the level and structure of the residual load[1], the correlation between flexibility potential and regional load or generation peaks, and the distribution of charging to the different locations (at home, at work, or other places). Thus, to fully comprehend the potential of EV charging flexibility in reducing peaks, a comprehensive regional analysis and quantification of the flexibility potential and its effects are crucial.

Two basic deployment strategies for deploying local EV charging flexibility can be distinguished. On the one hand, flexibility can be used to flatten the national residual load by reducing positive and negative peaks. That is, EV charging flexibility is used to reduce load during peak load situations and to absorb excess renewable generation during times of high generation. Such a deployment strategy aims to reduce system costs by not employing (or even investing in) expensive generation technologies and fully utilizing generated renewable electricity. An incentive scheme for such a deployment strategy would be the incentivization of flexibility deployment based on the uniform

[1] The residual load is the difference between total load and generation by intermittent resources.

pricing signals of the national electricity market. Alternatively, flexibility can be dispatched to smooth the regional residual demand. Such a deployment strategy aims to reduce the load on regional distribution grid components. This approach would reduce costs for the expansion of these grids.[2] Incentive schemes for such a deployment strategy would be, for example, quantity or price signals from distribution system operators according to the expected grid status. The goals of the deployment strategies may be partially opposed, and the question arises of how the two strategies affect the respective objectives.

In this research paper, we therefore first examine the regional evolution of residual load, load and feed-in peaks in Germany until 2045. Our analysis focuses on the spatial and temporal diffusion of EV charging, considering regional sigmoid transition pathways of EV adoption and regional and user-specific driving and load profiles. Our analysis is based on NUTS 3 regional resolution level data.[3] We then develop and implement a spatio-temporal optimization model for EV load flexibility based on the analysis. This model aims to quantify the potential of EV load flexibility of home charging in smoothing residual load time series and reducing load and feed-in peaks. We compare two different deployment scenarios: (1) using flexibility to flatten the national residual load time series, which corresponds to the use of flexibility based on price signals from the national electricity market, and (2) using flexibility on regional residual load and, thus, reduce the strain on regional distribution grid components.

EV charging is considered a major source of demand flexibility, as shifting charging operations can reduce peak loads and thus reduce the need for grid expansion. While some sources also note this at the transmission grid level (Gunkel et al., 2020; Amann et al., 2022), the impact of smart charging is predominantly analyzed at the level of the local distribution grid (e.g. Flataker et al., 2022). Powell et al. (2022) demonstrate that the flexibility of EV charging possesses not just a significant temporal component but also a geographical one, reflecting the propensity of EVs to move between locations

[2] Agora Verkehrswende et al. (2019) quantifies the investment costs in the low and medium voltage grid under the assumption of uncontrolled charging of EVs depending on the charging capacity and the number of electric cars with 23 to 72 billion € between 2020-2030.

[3] The Nomenclature of Territorial Units for Statistics (NUTS) is a hierarchical system for dividing European territory into territorial units. While, for example, NUTS 0 stands for states, NUTS 3 corresponds to smaller units within states, such as districts.

over the course of a day. They underscored the necessity for a comprehensive area-wide charging infrastructure to facilitate daytime charging, which could utilize surplus PV generation and avert the late afternoon peak load, as exemplified by workplace charging. Such conditions have direct implications for power system requirements in terms of storage and ramping needs or emissions. Given the residual load-smoothing potential of flexible end-uses, such as electric vehicle charging, there seems to be a general recognition in the European Union that local flexibility mechanisms are of significant interest for the operation of future distribution networks (CEER, Council of European Energy Regulators, 2020). Regulators have begun to put in place the regulatory framework to incentivize the provision of flexibility and its call-off by distribution system operators, which they are required to do by Article 32 of Directive (2019/944) as part of the clean energy package (Council of European Union and European Parliament, 2019).

However, while there is an elaborated stream of research analyzing the provision of regional flexibility from a market design perspective (Radecke et al., 2019; Rebenaque et al., 2023), to our knowledge, there is no research addressing the concrete added value of local flexibility use in contrast to centralized electricity markets, neither for demand-side flexibility in general nor for EV charging in particular. We attempt to fill this gap with a focus on the German power system at the national and regional levels.

From a system perspective, there are several studies that shed light on the transformation of the German energy and consumption sector until 2045 and beyond (e.g. Prognos et al., 2020; Burchardt et al., 2021; dena, 2021; Consentec et al., 2021; Kopernikus-Projekt Ariadne, 2021). The studies develop individual scenarios for possible pathways to reduce greenhouse gas emissions and to diffuse and use technologies, such as wind turbines, PV systems, or EVs, on the demand and supply side. While the specific numbers on installed capacity and electric vehicles differ, the emerging trends, a significant increase compared to today, are the same (dena, 2022). However, the studies only marginally touch on the regional perspective of the transition and the regional balance of supply and demand.

The regional matching of supply and demand for the German energy system is addressed by Kockel et al. (2022) and Kühnbach et al. (2021). Kockel et al. (2022) analyze the development of regional

residual loads in Germany on a spatio-temporal basis, related to an emission reduction of 95% by 2050 based on dena (2018). They note significant potential for demand-side flexibility, but do not specifically model or quantify it. Because the study only considers 2019, with very low EV penetration, and 2050, with penetration near 100%, the EV load is determined by a uniform distribution of regional demand based on regional vehicle counts. However, this approach is not appropriate for modeling EV penetration for the years in between, as it neglects regionally varying penetration rates. For EV charging, the same profiles are used for each region, abstracting from regional characteristics such as longer driving distances in rural areas compared to urban areas.

Kühnbach et al. (2021) focuses primarily on regionalized demand and the potential of demand response. In addition to analyzing regional supply and demand balancing, they examine the residual load-smoothing potential of flexible demand on a regional basis. They compare 2015 and 2030 and define indicators to measure supply-demand balance. They conclude that demand management is most effective in regions that frequently alternate between demand and supply deficits. However, the study lacks a comparison of regional results with a centralized energy system, and as in Kockel et al. (2022), the chosen scenario does not fit with Germany's recent climate protection goals of climate neutrality by 2045 (Deutscher Bundestag, 2021).

To be compatible with current German climate targets, we develop a scenario based on KN100 from dena (2021). In contrast to existing literature, our analysis focuses on the consistent regional and temporal modeling of EV charging demand and flexibility potentials. To this end, we model EV diffusion for 2019, 2030, and 2045 by utilizing the Bass model (Bass, 1969) that has been applied to EV diffusion in various countries in the literature (Becker et al., 2009; Won et al., 2009; Song, 2013; Zhu et al., 2017). We derive the load and flexibility profiles of EVs from the mobility patterns of the German Mobility Panel (MOP) (KIT - Institut für Verkehrswesen, 2021).

We address two key questions: To what extent can electric vehicle home charging flexibility reduce load and feed-in peaks at the national and regional levels? What are the impacts of the two different deployment strategies on national and regional residual demand curves, as well as load and feed-in

peaks? Besides answering these questions, this paper adds to the existing literature in multiple ways:

- Analysis of the spatio-temporal evolution of residual demand under a current scenario for Germany's energy transition pathway until 2045 with a focus on EV diffusion and load.
- Introduction and application of a method for modeling target-consistent regional and temporal diffusion of electric vehicles using sigmoid functions.
- Derivation of user- and region-specific driving, load and flexibility profiles for electric vehicles in Germany until 2045.
- Development and implementation of a model for spatio-temporal deployment of electric vehicle load flexibility under different objectives.

Concerning the development of future residual load, we find that positive and negative peaks in residual load increase over the years on the regional level and aggregated over Germany. The correlation between residual load and EV charging profiles is high in 2019 but decreases until 2045. This implies that the marginal utility of charging flexibility to reduce load peaks decreases over time, although the flexibility potential in absolute terms is increasing with growing EV adoption. We find that, especially in load- and PV-dominated regions, the nationally incentivized activation of flexibility can result in drastically higher regional demand peaks compared to a scenario without the use of charging flexibility. Our study shows that the two scenarios of flexibility activation can be contradictory in their effects: While the regional incentivization is less efficient in reducing peaks on the national level, the national incentivization leads to increased strain on local level. Our findings provide valuable insights into the challenges faced by regional grids and the development of strategies to harness EV flexibility to address these challenges.

The paper is structured as follows: In a first step (Section 2), regionalized diffusion curves for EV expansion from 2019 to 2045 and regionalized charging profiles for different user types are developed. Then a scenario of electricity demand development and renewable capacity expansion until

2045 is regionalized, and corresponding demand and renewable generation time series are presented (Section 3). In Section 4, a model for the regionalized optimization of EV charging flexibility is developed. The results (Section 5) address the estimation of residual demand time series for the years 2019, 2030, and 2045 on a regional and national level as well as the potential and effects of EV charging flexibility under two different deployment strategies. The paper concludes with a summary of the findings and their implications for the transformation of the power system and usage of EV charging flexibility.

2. Spatio-temporal expansion of private electric vehicles

This chapter focuses on the projection of regional expansion paths of electric vehicles and the development of a method to derive individual load and flexibility profiles for each region. Section 2.1 describes the applied method to derive regionalized transition pathways for electric vehicles. Each region reflects a NUTS 3 district of Germany. In Section 2.2, we develop load profiles for each region, distinguishing between different user types based on their charging locations and times.

2.1. Regional diffusion of electric vehicles

In recent years, several studies (e.g. Prognos et al., 2020; Burchardt et al., 2021; dena, 2021; Consentec et al., 2021; Kopernikus-Projekt Ariadne, 2021) presented development pathways for the future energy system and the transition to e-mobility in Germany. The "dena study - towards climate neutrality" projects 14 mil. electric vehicles in 2030 and 36 mil. in 2045 in its climate neutrality scenario "KN100" (dena, 2021). Also, in the summer of 2022, the German Federal Ministry for Economic Affairs and Climate Action announced that 15 mil. electric vehicles should be achieved by 2030 (German Government, 2022). Despite these national projections and targets, there is a lack of scenarios at the regional level. Regions in Germany are very heterogeneous, and it can be assumed that the penetration speeds with electric cars differ among them. Therefore, we aim at decomposing the national transition scenarios to the local level based on a NUTS 3 resolution, which is, for Germany, equivalent to individual districts.

Forecasting methods for the regional diffusion of technologies can be primarily categorized into agent-based, consumer choice, and diffusion rate and time-series methods (Ayyadi and Maaroufi, 2018). While methods of the first kind are simulation-based, simulating the interactions of agents and how these affect the market, consumer choice models depend on assumptions of consumer decisions about new technology according to certain characteristics (Kumar et al., 2022). Methods of the third kind rely on time series and diffusion rates to study technology diffusion. Existing research utilizing the latter methods primarily focuses on four models: Gompertz (Gompertz, 1825; Muraleedharakurup et al., 2010), Logistic (Kumar et al., 2022; Berger, 1981), Bass, and Generalised Bass (Bass, 1969) diffusion models. The Bass diffusion model fits our problem well because it can account for different speeds in the early and late stages of the diffusion, which is not the case for other models (Bass, 1969; Pavlidou, 2010). It has also been widely applied in the analysis of EV diffusion in other countries and for earlier years (Becker et al., 2009; Won et al., 2009; Song, 2013; Zhu et al., 2017). The Bass diffusion model and its transformation are written in equations (1) and (2) as a sigmoid function (Bass, 1969).

$$\frac{f(t)}{1-F(t)} = p + q\frac{A(t)}{m} = p + qF(t) \tag{1}$$

$$F(t) = \frac{A(t)}{m} = \int_0^T f(t)dt \quad withF(0) = 0 \tag{2}$$

The function $f(t)$ describes the likelihood of a purchase at time t with p being the probability of initial purchases at the start of the innovation ($t = 0$). p is referred to as the coefficient for innovators, while q is the coefficient for imitators. The two coefficients define the slope of the sigmoid function at the beginning and at the end. The cumulative diffusion level at time t $F(t)$ equals the cumulative number of adopters $A(t)$, which in our case reflects the number of EV owners divided by the total market size m, the total number of cars.

The diffusion level $F(t)$ in our approach is described as shown in equation (3).[4] The parameter t_0 is included in the function to take the beginning of the diffusion into account and to move the diffusion curve in time. Further, we introduce a scaling factor s. With the scaling factor, we ensure

[4]The transformation steps are depicted in Appendix A.

that the diffusion curve meets the maximum penetration rate in 2045. While improving the fit of the sigmoid function to the data points between 2019 and 2045, the scaling factor increases the maximum relative market potential in 2050 above 100%. Since our analysis focuses on the years until 2045, this is not an issue.

$$F(t) = s * \frac{1 - e^{-(p+q)(t-t_0)}}{1 + \frac{q}{p} e^{-(p+q)(t-t_0)}} \tag{3}$$

Fitting the curve

We derive our regional scenarios of electric vehicle diffusion by regional decomposition of the national scenario "KN100" of dena (2021), adjusted by the target of 15 million electric vehicles until 2030 defined by the German government (German Government, 2022). The development of regional scenarios using the Bass model is done in a two-step process, visualized in Figure 1.

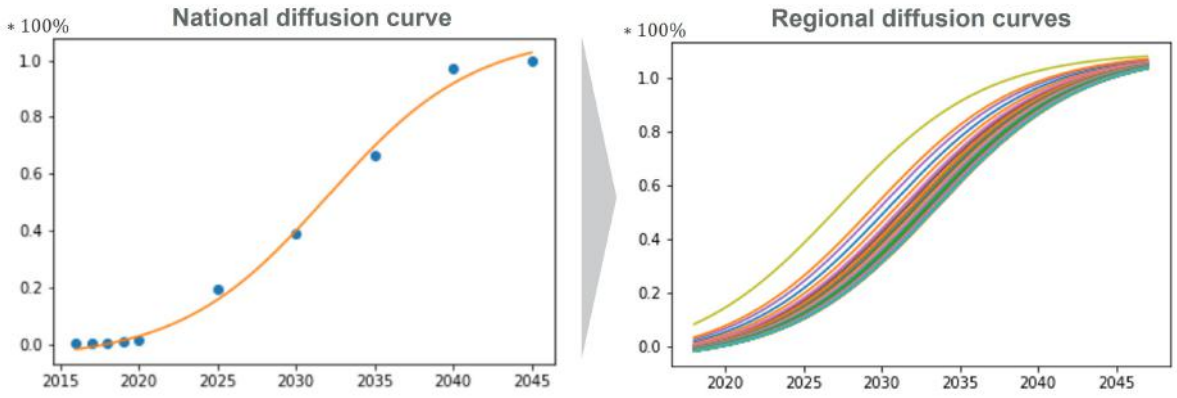

Figure 1: Development of regional Diffusion Curves

In the first step, the Bass function is fitted to the national scenario using the non-linear least squares (NLLS) method according to Newville et al. (2016). The left part of Figure 1 shows the rate of electric vehicles over time. The blue dots represent the penetration rate in the different years based on historic developments (until 2020) and the national scenario. The penetration rate of 42% in 2030 matches the number of 15 mil. electric vehicles, and a penetration rate of 100% corresponds to 36 mil. electric vehicles. The parameter s, the maximum relative market potential of electric vehicles, is also computed by the fitting method. The computed values for the estimates are: $\hat{s} = 1.096$, $\hat{p} = 0.203$ and $\hat{q} = 0.010$.

While the derived national diffusion curve is fitted to the historic national electric vehicle penetration, historic developments in the specific German regions can drastically differ. In the start year t_0=2020 (the last year regional data is available), every region has its individual position on the curve. Some regions are above the national average and some are below. Therefore, in a second step, we individually shift the national diffusion curve along the time axis for each NUTS 3 region to achieve the specific penetration level, as it is visualized in the right part of Figure 1. To calculate the regional EV diffusion levels in 2020 we use historical data of the EV fleet from 2017 to 2020 on postcode level, provided by the Kraftfahrt-Bundesamt (KBA) in two data sets (Kraftfahrt-Bundesamt, 2018b, 2019b, 2020b, 2021b and Kraftfahrt-Bundesamt, 2018a, 2019a, 2020a, 2021a). The EV diffusion levels reached in 2020 for each NUTS 3 region $F^{nuts3}(t = 2020)$ are calculated by dividing a region's total EV fleet EV^{nuts3}_{2020} by the ratio of the total region fleet $Cars^{nuts3}_{2020}$ to the total national fleet $Cars^{DE}_{2020}$ times the total German market size for EVs EV^{DE}.

$$F^{nuts3}(t = t_0) = \frac{EV^{nuts3}(t = t_0)}{EV^{nuts3}(t = 2045)} \tag{4}$$

$$with \quad EV^{nuts3}(t = t_0) = \frac{Cars^{nuts3}(t = t_0)}{Cars^{DE}(t = t_0)} * EV^{DE}(t = 2045) \tag{5}$$

To create diffusion curves for each NUTS 3 region, the derived national diffusion curve is moved along the time axis according to the time difference Δt between 2020 and the time t when the EV diffusion level for 2020 of the respective NUTS 3 region is reached on the national diffusion curves. Equation (6) describes the approach. Here, the parameters $\hat{m}$, $\hat{p}$ and $\hat{q}$ reflect the estimates of the national diffusion curve. The derivation of the formula, including Δt, can be found in Appendix B.

$$F^{nuts3}(t) = \hat{m} * \frac{1 - e^{-(\hat{p}+\hat{q})(t-t_0+\Delta t)}}{1 + \frac{\hat{q}}{\hat{p}} e^{-(\hat{p}+\hat{q})(t-t_0+\Delta t)}} \tag{6}$$

To get the total number of electric vehicles in each NUTS 3 region, the diffusion rates are multiplied by the total estimated market size of EVs for each NUTS 3 region. The latter is derived by multiplying the maximum estimated scenario value for EVs (EV^{DE}_{Y}) with the ratio of the total vehicle fleet of each NUTS 3 region in 2020 to the total national fleet according to equation (7). To ensure that the national target of EVs in a specific year is equal to the sum of all regional numbers

of EVs, a correction factor σ_y is used for scaling. The scaling factor adjusts the diffusion curves in a single point.

$$EV_y^{nuts3} = F(t)^{nuts3} * \frac{Cars_y^{nuts3}}{Cars_y^{DE}} * EV_Y^{DE} * \sigma_y \tag{7}$$

The result of the modeled diffusion of EVs is presented in Figure 2 for the years 2030 and 2045. In terms of consistency with the following sections, the historic distribution is visualized for the year 2019 instead of 2020. In the figure, the total number of EVs in every NUTS 3 region is normalized by the size of each region.

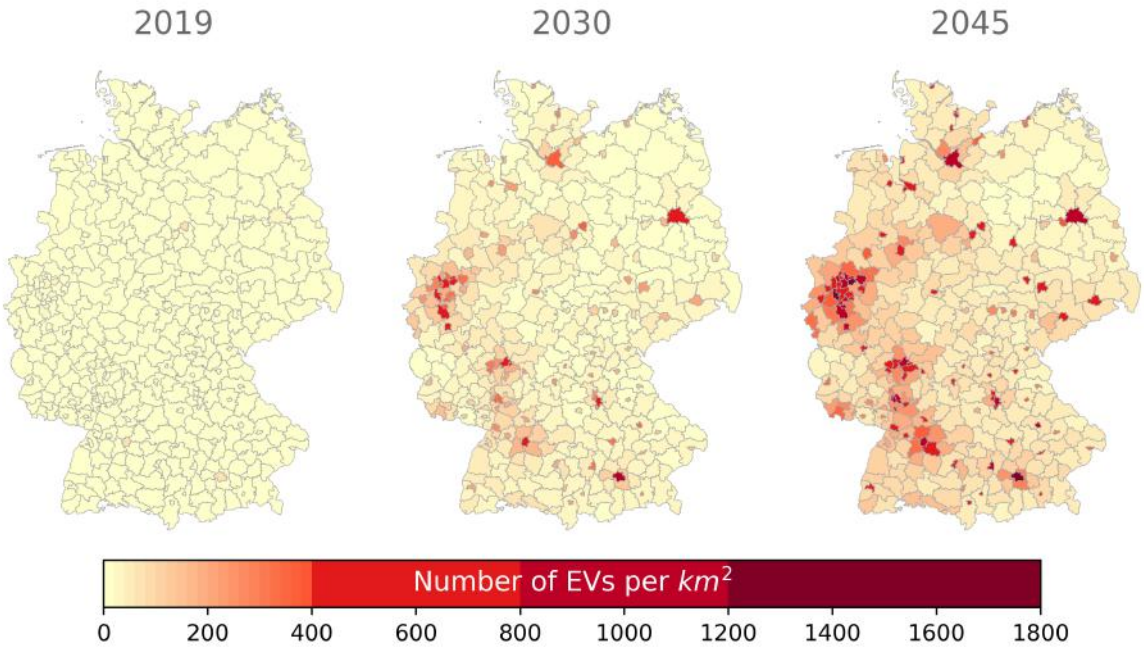

Figure 2: Number of electric vehicles in each NUTS 3 region for the years 2030 and 2045

In 2019, around 239 thous. electric vehicles do not lead to high penetration rates per square kilometer. In 2030 mainly bigger cities such as Hamburg, Berlin and Munich, as well as some areas in North-Rhine Westphalia, such as Dusseldorf, do have a significant amount of electric vehicles per square kilometer. Later in 2045, the western part of Germany and the Rhine-Main region are highlighted in red. Also, smaller regions, in terms of area but with a high population per square kilometer, have a high relative amount of electric vehicles.

2.2. User-specific load and flexibility profiles

The electricity demand of electric passenger vehicles is determined by their underlying driving patterns. For Germany, there are two major panels surveying the mobility behavior of households, *Mobility in Germany (MiD)* (infas et al., 2018) and the *German Mobility Panel (MOP)* (KIT - Institut für Verkehrswesen, 2021). While the MiD is updated every six years, the MOP has been updated annually since 1994. It is a survey-based longitudinal study of the mobility behavior of the German population. Besides household-specific information, it holds data on the households' individual trips, including timestamps, destinations, distances, and modes of travel. The panel categorizes about 14 thousand surveyed households according to ten settlement types, from small villages to metropolises. The dataset and information on the regional settlement structure enable the assignment of households and their respective mobility patterns to different regions. As a common assumption, we assume that the mobility behavior of EVs does not substantially differ from those of conventional passenger cars, and we assume the mobility patterns of vehicles remain constant until 2045. The detailed analysis of 500 thousand individual trips and car-based mobility patterns allows for deriving electric vehicles' energy demand and load profiles and the resulting inherent flexibility of their charging processes by user type, region, charging scenario, and day type for the years 2019, 2030, and 2045.[5]

Computation of regional differentiated load profiles

By projecting the historical mobility data on the years 2019, 2030, and 2045, average load profiles per vehicle are calculated, which are later scaled by the individual region's total counts of EVs.

The load profiles are calculated for different settlement types, charging scenarios, and day types (weekend and weekday) for each year considered. A total of six settlement types are distinguished, ranging from rural communities to large cities. The charging scenarios represent combinations of three potential charging locations (at home, at work, at other locations). The combinatorial approach results in seven scenarios, e.g., *charging at home and at work, but not at other locations.* In this way, a total of 252 profiles are distinguished.

[5] A brief descriptive analysis of the mobility data is given in Appendix C.

Starting from single trips, consecutive trips within a day are stacked into trip chains to derive the mobility patterns of individual cars in the form of binary time series indicating the standing and driving intervals of the vehicles, including their location. For the trips, the electricity demand is determined based on the distance traveled and the assumed EV fleet's average specific consumption of $0.21 kWh/km$ in 2019, $0.18 kWh/km$ in 2030, and $0.15 kWh/km$ in 2045 (dena, 2021). Assuming a charging power of $11 kW$ and an immediate start of charging upon arrival at a charging location, the energy demand is translated into profiles. Vehicles charge until the battery is full or a new trip begins. The average load profiles per vehicle are generated by aggregating all profiles and dividing them by the number of vehicles in the respective settlement type, charging scenario, and day type. As an example, the resulting profiles for medium-sized cities for the charging scenarios "charging at home" and "charging at home and work" for the year 2030 are shown in Figure 3. When vehicles can only be charged at home, a load peak is observed in the afternoon, while the load is more evenly distributed throughout the day when charging at home and work is possible.

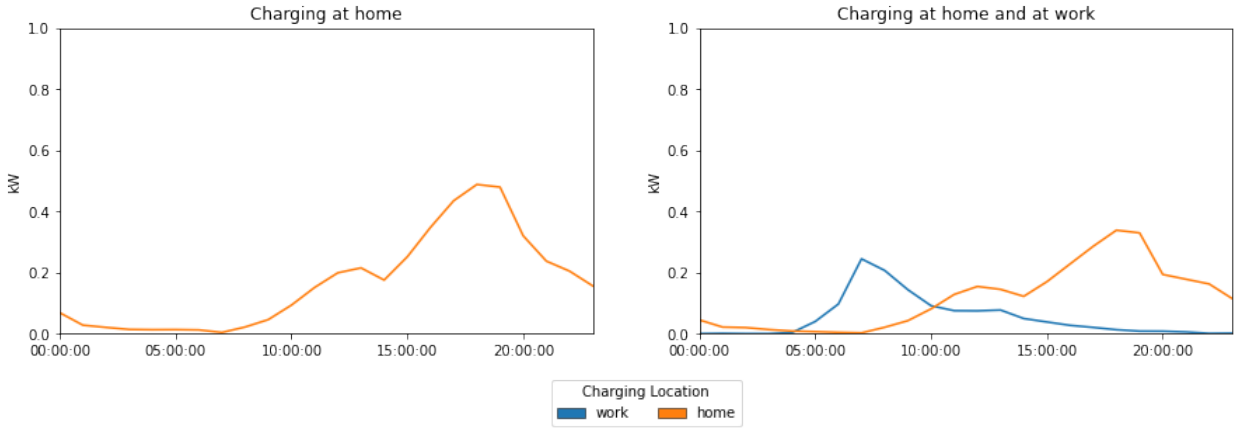

Figure 3: Selected load profiles for a medium-sized city in 2045

The final hourly load time series are composed of the standardized profiles and scaled by the respective vehicle counts determined in Section 2.1 for each NUTS 3 region. To this end, the regional settlement types are given by BBSR (2022). The proportions of the seven charging scenarios are derived from data on vehicle parking situations at home, distinguished by settlement type based on

dena and Prognos (2020)[6]. The scaled load profiles are then used in combination with the results from Section 3 to calculate the regional residual load curves in Section 5.

Computation of regional differentiated flexibility profiles

To model the home charging flexibility, we derive the flexibility potentials of the charging processes from the mobility patterns and the generated load profiles. The time series of flexibility potential become an input for the flexibility model (Section 4), which optimizes the load shifts for charging processes relative to the determined load profiles. Generally, we distinguish between positive and negative charging flexibility while focusing on uni-directional home charging only. Positive flexibility can reduce the load of charging compared to the load profile generated in the previous section. Thus, the positive flexibility potential in each hour is equivalent to the determined load profile. Negative flexibility, in turn, means load can potentially be increased in certain intervals. Therefore, the negative flexibility potential is limited upwards by the maximum available capacity. It is calculated as the difference between the generated load profile and the maximum available capacity in each hour if the vehicle is home. For computational reasons, the flexibility model does not model EVs individually, although this would ensure consistency in terms of EV flexibility provision: Car A reduces the load in hour X and increases the load in hour Y. Aggregating all flexibility profiles and centrally optimizing the deployment without restrictions would again lead to inconsistencies and, thus, overestimate the potential for smoothing the residual load: Car A reduces the load in hour X and car B increases the load in hour Y. To address this, we suggest a trade-off between an aggregated centralized, top-down approach and a fully decentralized bottom-up approach using clusters. The mobility patterns are divided into multiple clusters by clustering binary mobility patterns (at home, not at home) using k-medoids to ensure consistency within smaller segments of the observed trip chains. We then consider only the part of each trip chain's flexibility profile that is determined by each cluster centroid's mobility pattern, as conceptually shown in Figure 4.

[6]The shares of the different charging scenarios are depicted in Appendix D. We assume equal proportions within the two subgroups of charging scenarios that involve either at least partial home charging or no home charging.

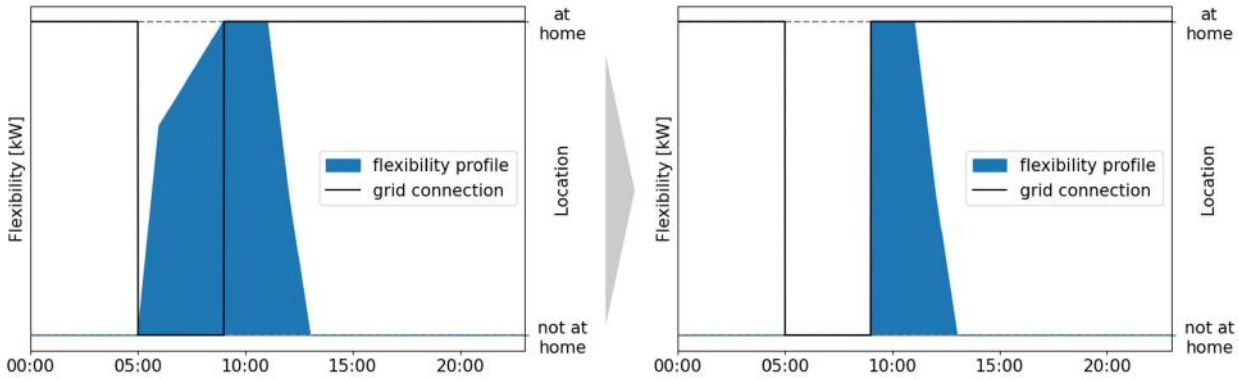

Figure 4: Concept for generating flexibility clusters

In our analysis, we find eight clusters as a suitable segmentation for the observed mobility patterns for weekdays and weekends. Figure 5 shows the resulting eight clusters.

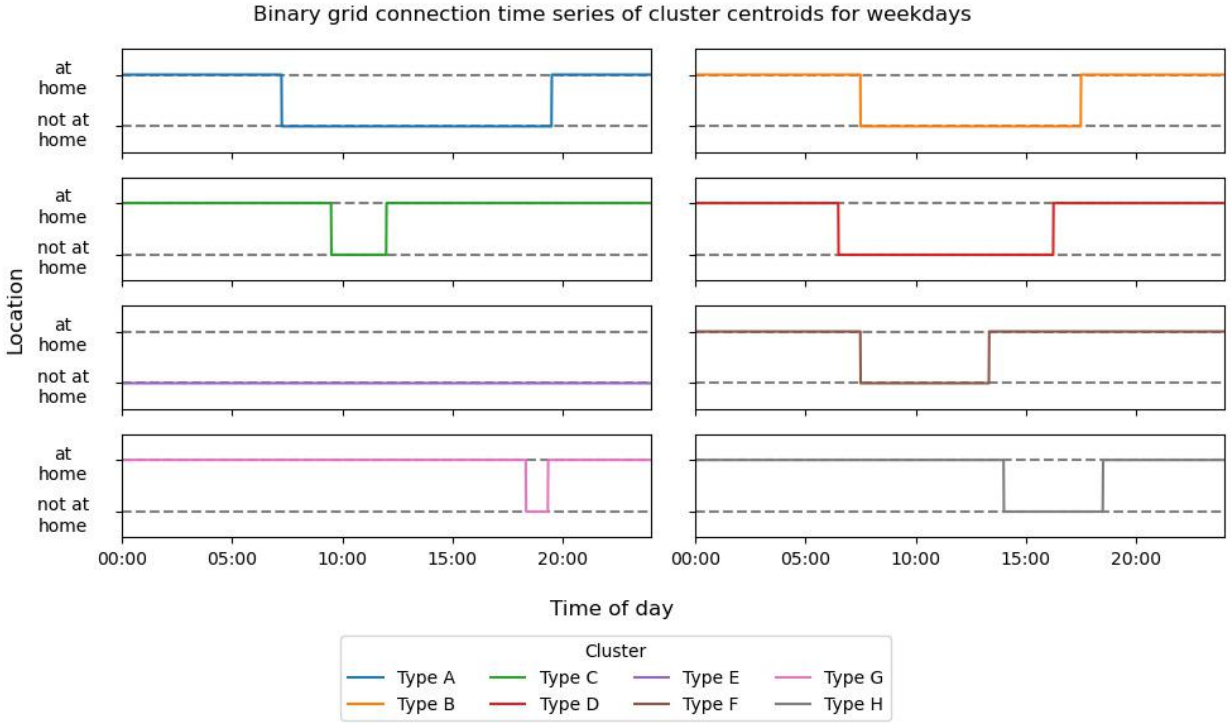

Figure 5: Flexibility clusters for weekdays

The resulting flexibility profiles for a medium-sized city and the year 2030 are shown in Figure 6. Since we only consider flexible charging at home, the positive flexibility is higher when vehicles can only charge at home. In general, the negative flexibility potential is much higher than the positive

flexibility potential, as charging is generally only carried out over short periods in relation to the idle times of the vehicles.

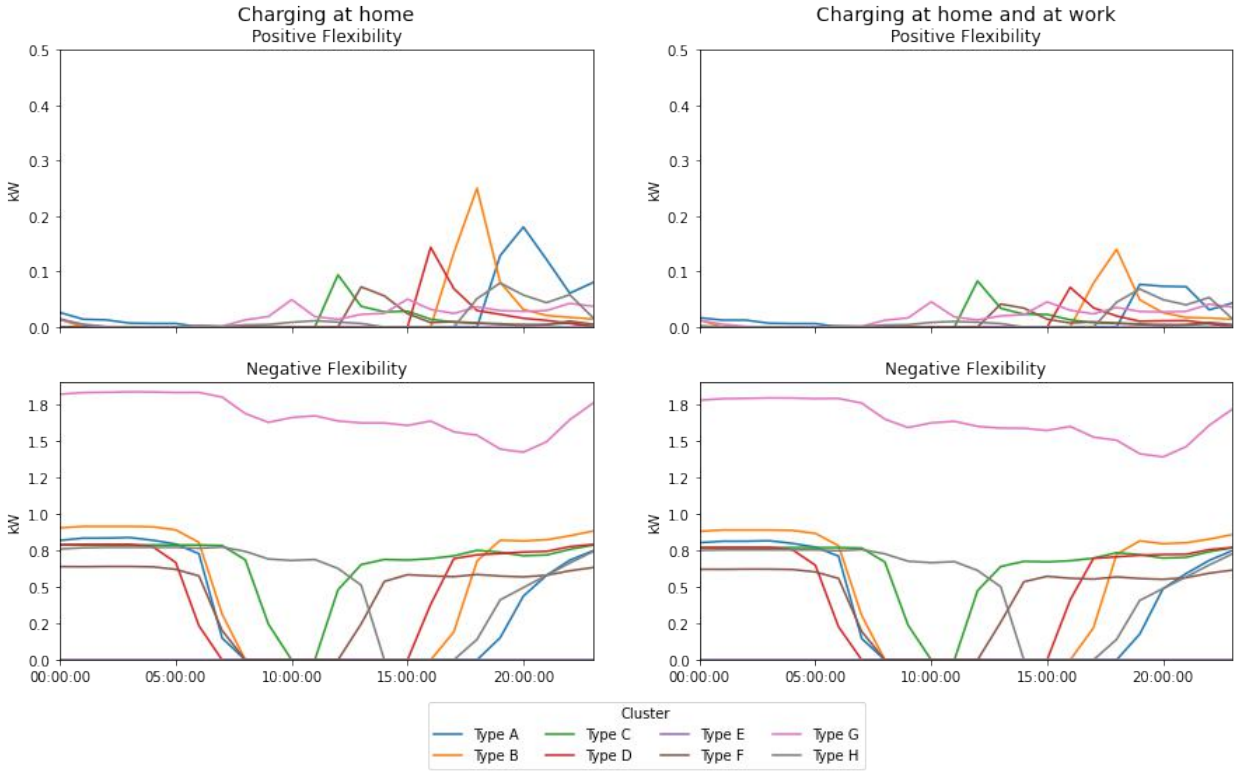

Figure 6: Selected flexibility profiles for a medium-sized city in 2045

The final flexibility time series for each NUTS 3 region are composed the same way as the load profiles. We assume that all households charging at home are willing to provide flexibility.

3. Regionalization of demand and supply

In order to examine the potential of using EV home charging flexibility for smoothing national and regional residual demand, we derive regional time series for electricity demand from the other consumption sectors in Section 3.1 and electricity generation from renewable energy sources in Section 3.2. Both sections focus on the spatial distribution to NUTS 3 regions first and then derive corresponding profiles.

3.1. Electricity demand

Spatial distribution of annual demand

Consistent with the EV market development, we adopt the electricity demand development of the remaining consumption sectors until 2045 from the "KN100" scenario from dena (2021). Table 1 shows the assumed annual evolution of demand by consumption sector and application.

Table 1: Annual electricity demand by sector and application in TWh

Sector	Application	2019	2030	2045
Households	SLP[1]residential	121	119	116
	Heat residential	6	20	29
	Light trucks	0	0	2
Small-scale Industries, Trade and Services	SLP commercial	133	129	118
	Heat commercial	9	21	28
	Base load	4	5	6
	Heavy trucks	0	1	2
	Light trucks	0	2	11
Industry	Heat commercial	4	9	12
	SLP commercial	17	16	19
	Base load	206	241	285
	Heavy trucks	0	5	10
	Light trucks	0	1	3
Rail transport		12	20	24
Conversion sector		8	8	8
Passenger cars[2]		1	34	58
Total		522	625	732

[1] standard load profile [2] The allocation of the demand from EVs is discussed in Section 2. Values deviate from dena (2021) due to updated government targets (15 mil. EVs in 2030).

The spatial allocation of the demand is done in two steps. In the first step, distribution keys, matching the sector-specific demand to the federal states, are derived based on data from Länderarbeitskreis Energiebilanzen (2022).[7] In the second step, sector-specific demand distribution keys to the regions within the federal states are derived. These are based on regional characteristics, such as residents, employees in the tertiary industry, income, and gross value added, taken from VWG (2022a) and VWG (2022b). Table 2 shows the weighting factors of these characteristics

[7] A detailed discussion of the approach and the derived distribution keys are presented in Appendix E.

to allocate the demand of the individual sectors from the federal states to regions. The weighting factors are chosen similarly to BNetzA (2020).

Table 2: Annual electricity demand by sector and application in TWh

Sector	Allocated by	Weighting factor
Households, rail transport	Residents	90%
	Income	10%
Small-scale Industries,	Employed in sector	20%
Trade and Services	Gross value added in sector	80%
Industry, conversion	Gross value added in sector	100%

Temporal distribution of regional demand

To derive the temporal distribution of demand, time series are determined for the individual applications, which are used to distribute the spatially distributed annual demand over the year. Four categories can be distinguished when creating our regional demand time series: Standard load profiles, time series for mobility applications, time series for heat generation, and applications for which we assume a constant power consumption. The standard load profiles (SLP) for household consumption ("H0") and commercial consumption ("G0") are taken from VDEW (1999). The daily profiles are available separately by day of the week (Monday-Friday, Saturday, Sunday/holidays) and by season (Summer, Winter, Transition) and are matched to the calendar year 2015. The profiles for light and heavy electric trucks are taken from ENTSO-E (2022b). The daily profiles are available, separated by Monday-Friday and Saturday-Sunday, and are matched based on this distinction to the calendar year 2015. Due to the temperature dependency of the heat generation profiles, they are calculated for each region separately. To calculate the profiles for households, we use the standardized profiles for heat pump electricity consumption as a function of time of day and outdoor temperature from SWM (2022) as well as regional temperature data for 2015 from Copernicus Climate Change Service (2020). For electricity demand from commercial consumers for heat generation, we use the profile data from Ruhnau and Muessel (2022) and match it with temperature data for 2015. Last, we assume uniform consumption over the year for the base load, rail transport and conversion applications. Figure F.2 in Appendix F illustrates the different profiles.

3.2. Electricity generation

Spatial distribution of annual renewable electricity capacities

As a starting point, existing capacities in 2022 of onshore wind, rooftop PV, large-scale PV and hydropower are spatially distributed according to the Marktstammdatenregister (BNetzA, 2022). Offshore wind capacities are located in a separate offshore region and are not spatially distributed. For the future development of each technology, the methods described in the network development plan 2023 (German TSOs, 2022) are reproduced using regional capacity potentials from Ebner et al. (2019). For 2045, the announced capacity targets within the so-called "Easter package" (Bundesrat, 2022) were assumed: 160 GW onshore wind, 200 GW large-scale and rooftop PV each.

For onshore wind, the distribution to regions is done according to the relative capacity potentials in the federal states compared to the total potential of Germany. As soon as the 2% target for each federal state is reached, the relative distribution factor in this federal state is devalued by 50%. The 2% area target thus represents a threshold value above which less area may be available for wind energy use in a federal state, thus slowing down the expansion. The remaining net expansion is then further distributed to the federal states in an iterative procedure based on the relative distribution of the respective potential. Based on the capacity assigned to each state, the capacity is further distributed to the NUTS 3 regions according to the relative potentials.

For the regional expansion of large-scale PV capacities until 2045, the regional potential areas for each federal state and the NUTS 3 regions are used as well. The target capacities for each federal state according to German TSOs (2022) are distributed by the weighted regional potentials. This is done by using a modification of the potentials. The potential area in the federal state with the highest average yield (Baden-Württemberg) is valued twice as high as the potential area in the federal state with the lowest average yield (Lower Saxony). For rooftop PV installations, the approach is postcode-specific. A constrained growth function is derived for each postcode using the change in existing installations to date and the maximum potential. This function is linear until 50% of potential is reached, and then approaches the potential limit asymptotically. This approach follows the observation that past additions have been largely linear. However, after a certain point, it decreases due to adding less suitable areas and slowly approaching the potential limit.

For hydropower, only existing capacities are regional distributed. No additional expansion is assumed.

Temporal distribution of regional renewable electricity generation

Generation profiles for the spatially distributed renewable capacities are based on the COSMO-REA6 weather data of the year 2015 provided by HErZ, Hans-Ertel Centre for Weather Research (University of Bonn - Germany) and DWD, Deutscher Wetterdienst (2022). The data set contains information regarding wind speed, temperature and solar irradiation. With these data, in-feed profiles for rooftop and large-scale PV are computed by replicating the method described in Huld et al. (2010). For onshore and offshore wind, power curves for standard wind turbines are utilized in combination with wind speed data. Feed-in time series for hydropower equal the historic time series from ENTSO-E (2022a).

4. Modelling electric vehicle charging flexibility

By aggregating the results of the previous sections, regionalized residual load time-series are computed. On the national level, positive peaks imply the utilization and steep ramping of (and the necessity of investment in) expensive dispatchable generation units. In contrast, negative peaks imply an excess of renewable energy generation. On the regional level, both positive and negative peaks put strain on distribution grid components such as transformers. Consequently, residual load curves should be smooth and close to zero. Electric vehicle charging represents one source of flexibility potential. We develop an optimization model for the deployment of regional flexibility of electric vehicles. In the model, we distinguish between two deployment strategies. Under the first strategy, the regional flexibility potential is used to flatten the corresponding regional residual load curves by reducing positive and negative peaks. This is our basic model, described in Section 4.1. Under the second strategy, the model is adjusted according to Section 4.2. Here, the flexibility potential of home charging processes is aggregated to flatten the national residual load curve instead.

4.1. Flexibility on regional level

The smoothing of the residual load has two objectives. First, to minimize the absolute distance to zero in every time step, and second, to minimize peaks. The objective functions in Equation (8) combines these by minimizing the square absolute value of the residual load. On a regional level, this optimization logic represents the minimization of grid expansion costs, which becomes necessary, especially when large positive or negative peaks occur. On the national level, the generation costs are to be minimized, which become disproportionately more expensive during positive peaks, which serves as a justification for the quadratic optimization approach. The objective function contains the adjusted residual load RL as a variable, which has two dimensions. One temporal $t \in T$ and spatial $n \in N$. The set T contains the 8760 hours of a year, and the set N contains all NUTS 3 regions of Germany.

$$\min z = \sum_{t}^{T} \sum_{n}^{N} |RL_{t,n}|^2 \tag{8}$$

The adjusted residual load curve $RL_{t,n}$ equals the residual load curve before load shift $rl_{t,n}$ plus the usage of load shift (LS), as it is shown in Equations (9) and (10).

$$RL_{t,n} = rl_{t,n} + \sum_{t_1}^{T} \sum_{u}^{User} (LS_{t_1,t,n,u} * ts^{max}_{t_1,t,u}) \quad \forall t \in T \wedge n \in N \tag{9}$$

$$with \quad LS_{t,t_1,n,u} = LS^{neg}_{t,t_1,n,u} - LS^{pos}_{t,t_1,n,u} \tag{10}$$

The variable LS has two time-dimensions and is defined for every region n and every user type $u \in User$. Furthermore, the variable can be decomposed into a positive part LS^{pos} and a negative part LS^{neg}. Negative flexibility here means that the load increases so that the residual load moves upwards. Positive flexibility reflects load reduction. For every user type s, the binary parameter $ts^{max}_{t_1,t,u}$ defines whether load shifting is possible from time step t_1 to time step t.

With the following two Equations (11) and (12), it is ensured that the maximum LS potential is not exceeded in every time step t, in every region n and for every user type u. Two equations are necessary to distinguish between a positive and a negative flexibility potential (see Section 2.2).

$$\sum_{t}^{T}(LS^{pos}_{t,t_1,n,u} * ts^{max}_{t_1,t,u}) \leq P^{max,pos}_{t_1,n,u} \quad \forall t_1 \in T \wedge n \in N \wedge u \in User \tag{11}$$

$$\sum_{t}^{T}(LS^{neg}_{t,t_1,n,u} * ts^{max}_{t_1,t,u}) \leq P^{max,neg}_{t_1,n,u} \quad \forall t_1 \in T \wedge n \in N \wedge u \in User \tag{12}$$

The last Equation (13) ensures that shifted energy is balanced for every user type and region within a fixed period of 24 hours. For every from-to relationship (amount of energy shifted from t to t_1), the sum has to equal zero.

$$\sum_{t_1}^{T}(LS_{t,t_1,n,u} * ts^{max}_{t_1,t,u}) = 0 \quad \forall t \in T \wedge n \in N \wedge u \in User \tag{13}$$

After the optimization of the use of flexibility, new residual loads are computed.

4.2. Flexibility on national level

To use the flexibility potential of home charging processes to flatten the national residual load curve, two equations of the basic model are adjusted. First, the residual load curve in the objective function (8) has no regional dimension anymore (Equation 14).

$$\min z = \sum_{t}^{T} |RL_t|^2 \tag{14}$$

Second, flexibility from all NUTS 3 regions and all user types is aggregated to smooth the national residual load curve. Instead of Equation (9), we formulate the following equation to compute the new national residual load curve.

$$RL_t = rl_t + \sum_{t_1}^{T}\sum_{u}^{User}\sum_{n}^{N}(LS_{t_1,t,n,u} * ts^{max}_{t_1,t,u}) \quad \forall t \in T \tag{15}$$

All other model equations stay the same as described in the previous section.

5. Analysis and results

Based on the methodologies and data presented in previous sections, we conduct a thorough analysis of the characteristics of regional and national residual load curves, and evaluate the impact of two deployment strategies for home charging flexibility. This section is divided into two parts. The first part, Section 5.1, focuses on analyzing residual load curves, aiming to answer two primary questions. How do regional residual loads develop over time? And what is the relationship between the load profiles of electric vehicles and regional residual load curves?

In Section 5.2, we analyze two deployment strategies for the flexibility provided by electric vehicles. We differentiate between national-oriented and regional-oriented activation of flexibility and use the presented optimization approach to answer the following question: What is the effect of different strategies for activating the flexibility offered by electric vehicles on regional and national residual load curves?

5.1. Residual load analysis

We categorize regions into three distinct clusters: Photovoltaic (PV)-dominated, wind-dominated, and load-dominated regions. The clustering is based on two dimensions: the average regional ratios of wind and PV feed-in to the average load, normalized by the maximum ratio across all regions in 2045. The clustering results are presented in Figure 7. A region is deemed load-dominated if both dimensions have a normalized value smaller than 0.20. A region is considered wind-dominated if it has a normalized wind-to-load ratio greater than 0.20 and greater than the PV-to-load ratio. The definition for PV-dominated regions follows the same logic.

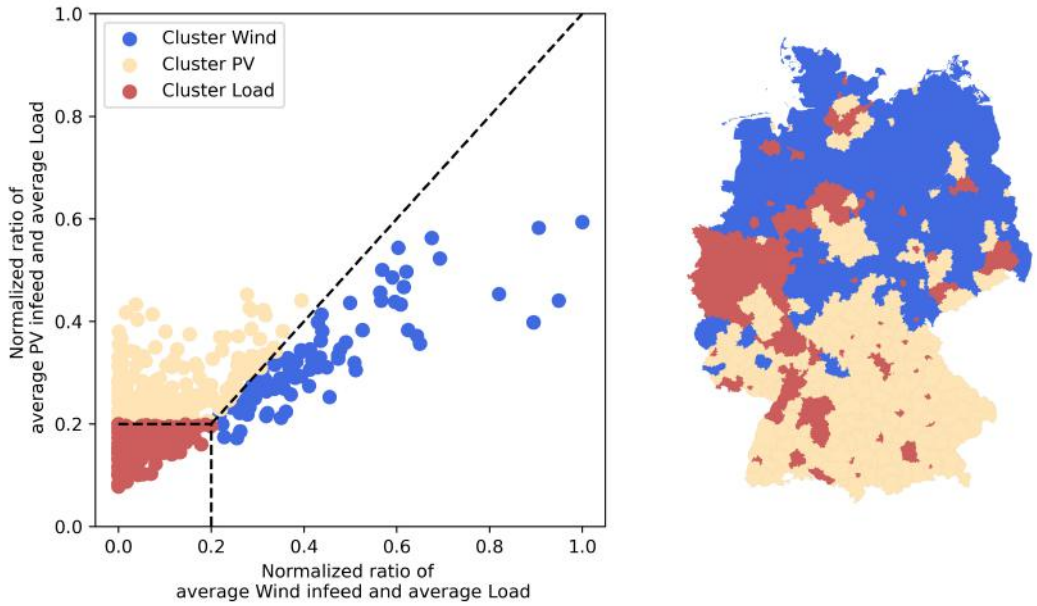

Figure 7: Clustering of the NUTS 3 regions

The wind-dominated regions are primarily situated in the northern part of Germany and consist of 98 NUTS 3 regions, covering an area of 157,753 square kilometers, equivalent to 44% of the total land area of Germany (357,588 square kilometers). The PV-dominated regions are located predominantly in the southern region of Germany, particularly in Bavaria. These 166 NUTS 3 regions have a total area of 140,332 square kilometers, accounting for 39% of Germany's land area. Load-dominated regions are primarily located in Germany's western and southwestern regions and include major urban areas such as Berlin, Hamburg, and Munich. This cluster consists of 137 NUTS 3 regions and has a total area of 59,666 square kilometers, accounting for 17% of Germany's land area. The clusters differ not only in terms of load, wind and PV generation ratios but also, for example, in terms of population density and number of EVs. Both are high in load regions and low in wind regions. Furthermore, individual regions within a given cluster also possess distinct characteristics in terms of parameters such as population density, renewable energy capacity, and adoption of electric vehicles. A detailed account of the distribution of regional properties for and within each cluster is provided in Appendix G.

Boxplots are computed for the three clusters and Germany to compare the properties of the residual load curves for the years 2019, 2030, and 2045 without considering flexibility. The results are presented in Figure 8.

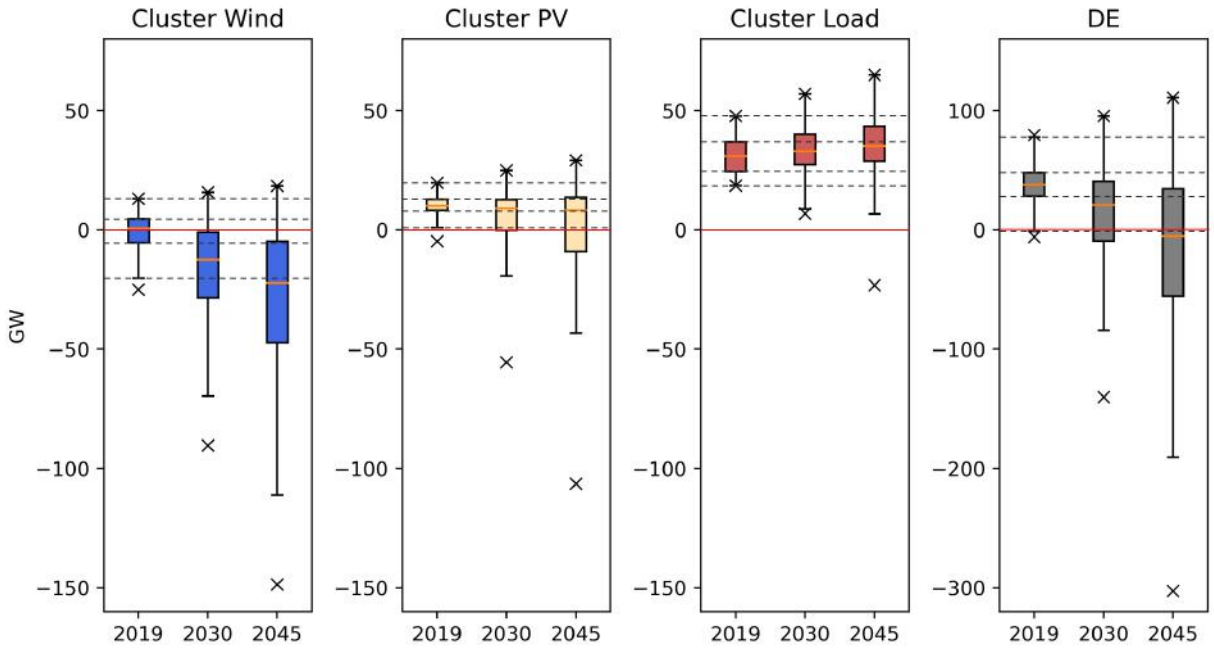

Figure 8: Comparison of regional residual load curves prior to the activation of flexibility

Note: The minimum and maximum values are represented by crosses. The median is depicted by the orange line, while the colored box between the lower and upper quantiles represents 50% of all values. The maximum whiskers are equal or lower to 1.5 times the Inter-Quartile Range (range of the colored box)

Regarding the **Cluster Wind**, the majority of residual load curve values show a decrease from 2019 to 2045. The median of the residual load curve decreases from 0.7 GW in 2019 to -12.4 GW in 2030 and further to -22.2 GW in 2045. The increased dependence on the weather for electricity generation leads to an increase in the variance of the residual load curve. The distance between the minimum and maximum values of the boxplot, a measure of dispersion, increases by 178% from 2019 to 2030 and by 338% from 2019 to 2045. This increase is attributed to the significant expansion of wind capacities relative to electrical load growth. The minimum values of the residual load curve increase from -25.0 GW in 2019 to -148.6 GW in 2045, while the maximum value increases by 41% from 13.1 GW in 2019 to 18.5 GW in 2045. The **Cluster PV** displays relatively stable properties for the residual load curve, with a slight decrease in the median from 10.1 GW in 2019 to 8.2 GW

in 2045. Similar to the wind-dominated cluster, the variance of the residual load curve increases, albeit to a lesser extent, due to the weather-dependent electricity generation and the limited impact of load. The properties of the residual load curve in **Cluster Load** display a different trend. The median increases from 30.9 GW in 2019 to a value of 35.2 GW in 2045, an increase of 14%. The maximum value of the residual load increases by around 36%, and the minimum value reduces from 18.5 GW in 2019 to -23.2 GW in 2045. The addition of new electric loads from electric vehicles and heat pumps in these regions is offset by the effect of rooftop PV expansion. As the peak demand occurs in the evening while the maximum feed-in from rooftop PV occurs at noon, the minimum and maximum values of the residual load curve diverge.

The residual load curve in Germany (**DE**) displays characteristics similar to those of the renewable-dominated clusters, as they represent a larger share of residual load. Additionally, the German residual load curve includes Offshore Wind feed-in, which is roughly correlated with the wind-dominated cluster.

Correlation between residual load and electric vehicle load curves

Besides the ratios of renewable feed-in and load, the three clusters differ regarding the correlation between residual load and the electric vehicle load curves. Table 3 shows the coefficients of correlation for the three clusters and the years 2019, 2030 and 2045.

Table 3: Correlation between residual load and electric vehicle load curves

Cluster	**2019**	**2030**	**2045**
Cluster Wind	0.08	-0.19	-0.25
Cluster PV	0.29	-0.21	-0.27
Cluster Load	0.74	0.46	0.11

The coefficients of correlation highlight that the residual load in the load-dominated cluster correlates most with the electric vehicles load profile. However, the correlation almost vanishes until 2045, caused by the penetration of rooftop PV applications and the electrification of further applications like heating or industrial processes. The residual load becomes less dominated by residential applications in the evening. The increasing weather dependency of electricity generation and a low

share of load compared to renewable feed-in is the reason for the lower correlation in 2019 and even negative correlation in 2045 in the other two clusters.

This development is relevant for the use of EV charging flexibility to reduce the residual demand. Today, especially in Cluster PV and Cluster Load, there would be a strong incentive to shift the load of EV charging to counter the high correlation with the residual load peaks. In 2045, however, especially in Cluster Wind and Cluster PV, EVs tend to be charged when the residual load is low (or negative). This development implies that the marginal utility of charging flexibility to reduce load peaks is decreasing over time, although the flexibility potential is increasing in absolute terms with growing EV adoption.

5.2. Flexibility of electric vehicles

This section provides a detailed analysis of two deployment strategies for utilizing the flexibility provided by electric vehicles. The objective of the analysis is to understand the impact of these strategies on the residual load curves at both national and regional levels. We distinguish two deployment strategies: First, we use flexibility to flatten the regional and, second, the national residual load curve. In the following, we use the formulations of "nationally incentivized" and "regionally incentivized" flexibility deployment for the use of the two deployment strategies. The optimization model outlined in Section 4 is used for the analysis. The properties of the resulting regional and national residual load curves for the years 2030 and 2045 are evaluated and compared.

Characteristics of the activation of flexibility

Figure 9 illustrates the model results for a single region with a temporal resolution of 48 hours. The figure highlights the differences in the shape of the residual load and load shifting between the two optimization schemes. For example, the charging process for user type C is shifted to hour 27 in the regional scheme but to hour 10 in the national scheme. The use of flexibility is mainly limited by the positive flexibility potential, as depicted by the dotted lines.

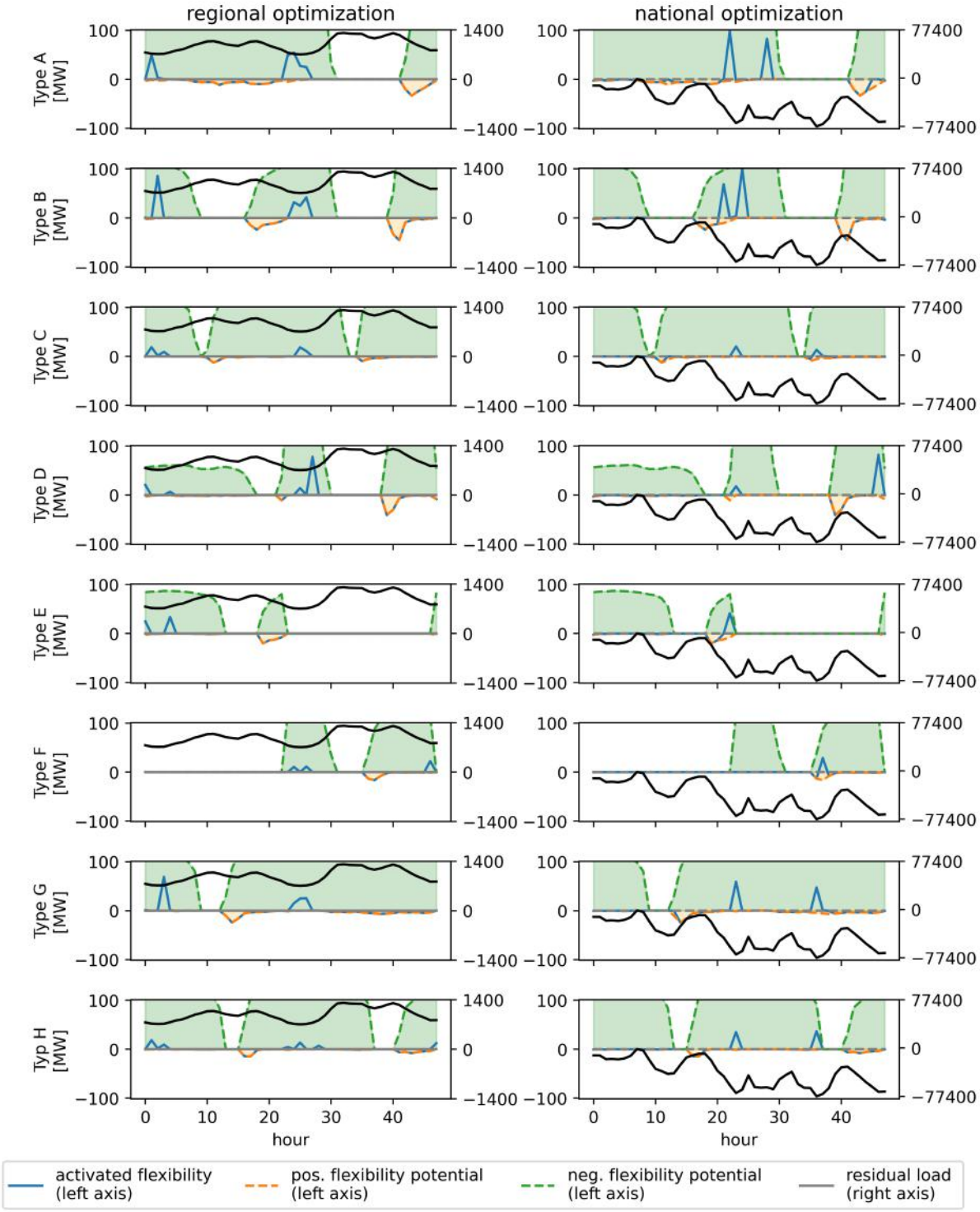

Figure 9: Optimal activation of flexibility in region DE111 (Stuttgart)

Note: The left column of the figure shows the results of the regional optimization and the right column shows the results of the national optimization. The residual load before the activation of flexibility (regional on the left and national on the right) is depicted using a black line, and the change of charging processes for user types A to H are shown in blue.

Model results on national level

The mechanisms for activating flexible charging processes impact the properties of the national residual load curve. In Figure 10, the residual load curves after regional and national incentivized activation of flexibility are compared to the residual load curve before the use of flexibility. This is done for the years 2030 and 2045.

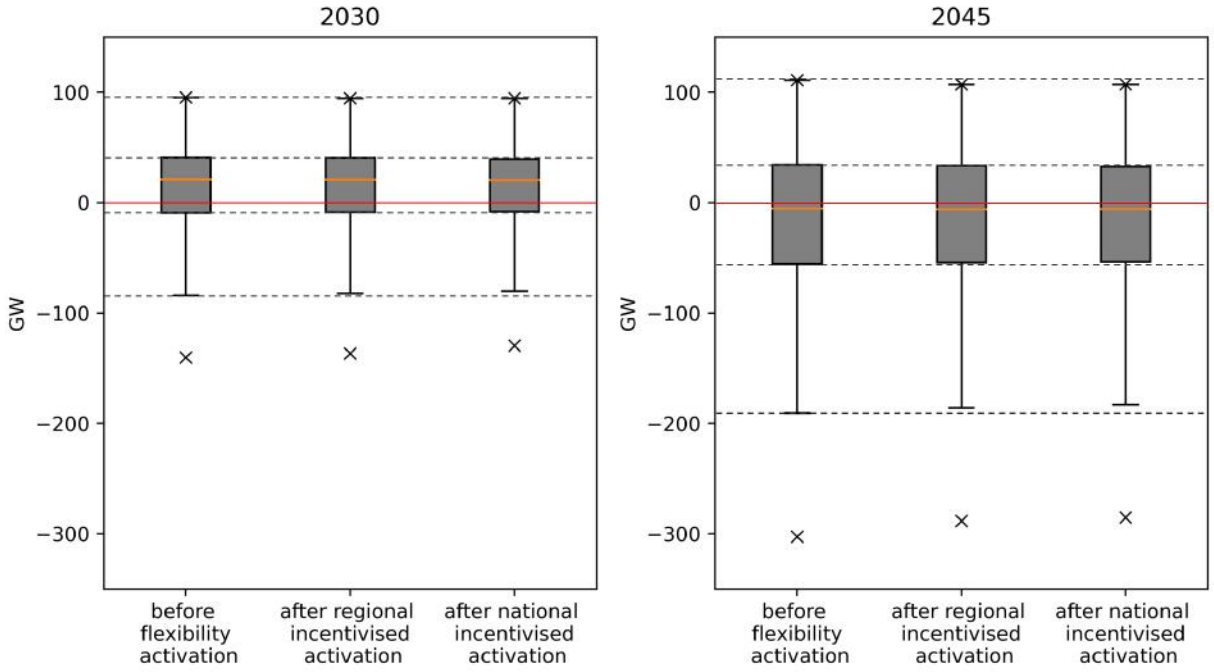

Figure 10: Properties of the national residual load curve before and after the use of flexibility

For both years, the range between the minimum and maximum values, as well as the absolute value of the peak change to a small extent through both national and regional incentivization of flexibility. However, national incentivization has a greater impact compared to the regional approach. In 2030, regional incentivization decreases the range between the minimum and maximum values by 1.9%, while national incentivization decreases this range by 4.8%. Before the use of flexibility, the negative peak surpasses the positive one in absolute terms. Regional incentivization reduces the peak by 2.6%, and national incentivization reduces it by 7.5%. These characteristics observed in 2030 can also be seen in 2045, but with higher values and a greater variance of the residual load. The use of flexibility reduces the absolute value of negative peak demand. The minimum changes

from -303 GW to -288 GW (-5.0%) with the regional approach and to -285 GW (-5.9%) with the national approach, while the maximum is only reduced by 4 GW (-3.6%) in both cases.

Model results on regional level

We calculate imbalance ratios to analyze the effects of the two flexibility deployment strategies on the regional feed-in and load peaks. These are defined as the positive or negative peaks in each region's residual demand divided by the respective regional total load and generation over a year.[8] The imbalance ratio can be formulated in a positive (PIR_r), negative (NIR_r) and an absolute (AIR_r) way (see Eq. (16) to (18)). Dividing the maximum amount of power needed in both the positive (RE deficit) and negative (RE surplus) direction in each region by total load and generation allows us to analyze and compare the development of peaks for the heterogeneous regions. Comparing the Imbalance Ratios before and after flexibility activation, we are able to quantify how flexibility changes the altitude of the load and feed-in peaks.

$$PIR_r = \frac{\max\limits_{h \in H}(residualload_{h,r})}{\sum_{h=1}^{8760}(totalload_{h,r} + generation_{h,r})} * 1000 \quad \forall r \in R \tag{16}$$

$$NIR_r = \frac{\min\limits_{h \in H}(residualload_{h,r})}{\sum_{h=1}^{8760}(totalload_{h,r} + generation_{h,r})} * 1000 \quad \forall r \in R \tag{17}$$

$$AIR_r = \max\left(|PIR_r|, |NIR_r|\right) * 1000 \quad \forall r \in R \tag{18}$$

Figure 11 visualizes the change of the imbalance ratios after the national and regional incentivized activation of flexibility in each region for the year 2030. Figure 12 shows the results for the year 2045. As reference values in both figures, highlighted in gray, the peaks in 2019 are normalized to the load and generation of 2030 and 2045, respectively.

[8] The use of this evaluation variable follows Kühnbach et al. (2021).

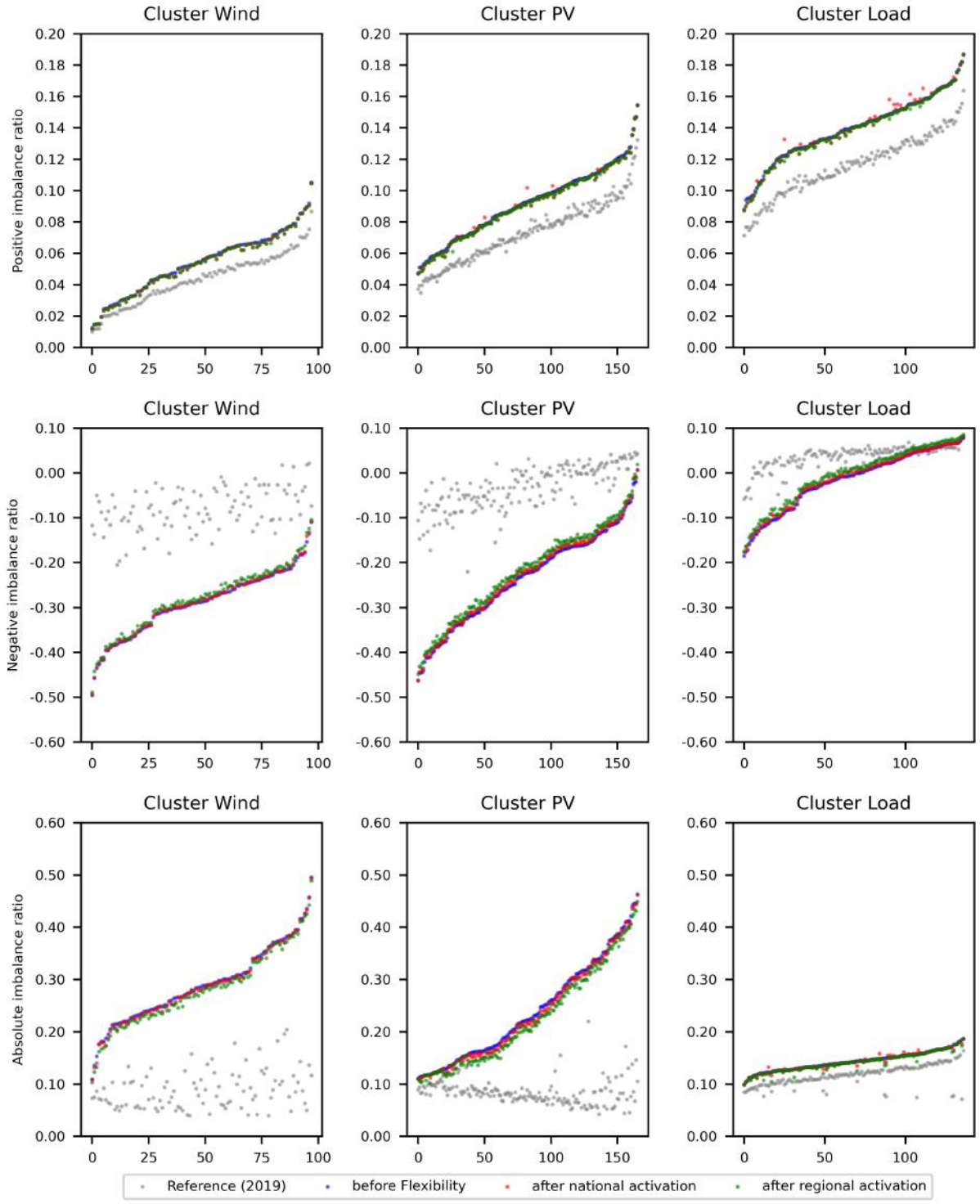

Figure 11: Imbalance ratios before and after the use of flexibility in 2030

Note: The x-axis represents the regions in each cluster. In each of the nine sub-figures, the imbalances before flexibility are sorted in ascending order. The imbalance ratios after the activation of flexibility are then matched to the corresponding region.

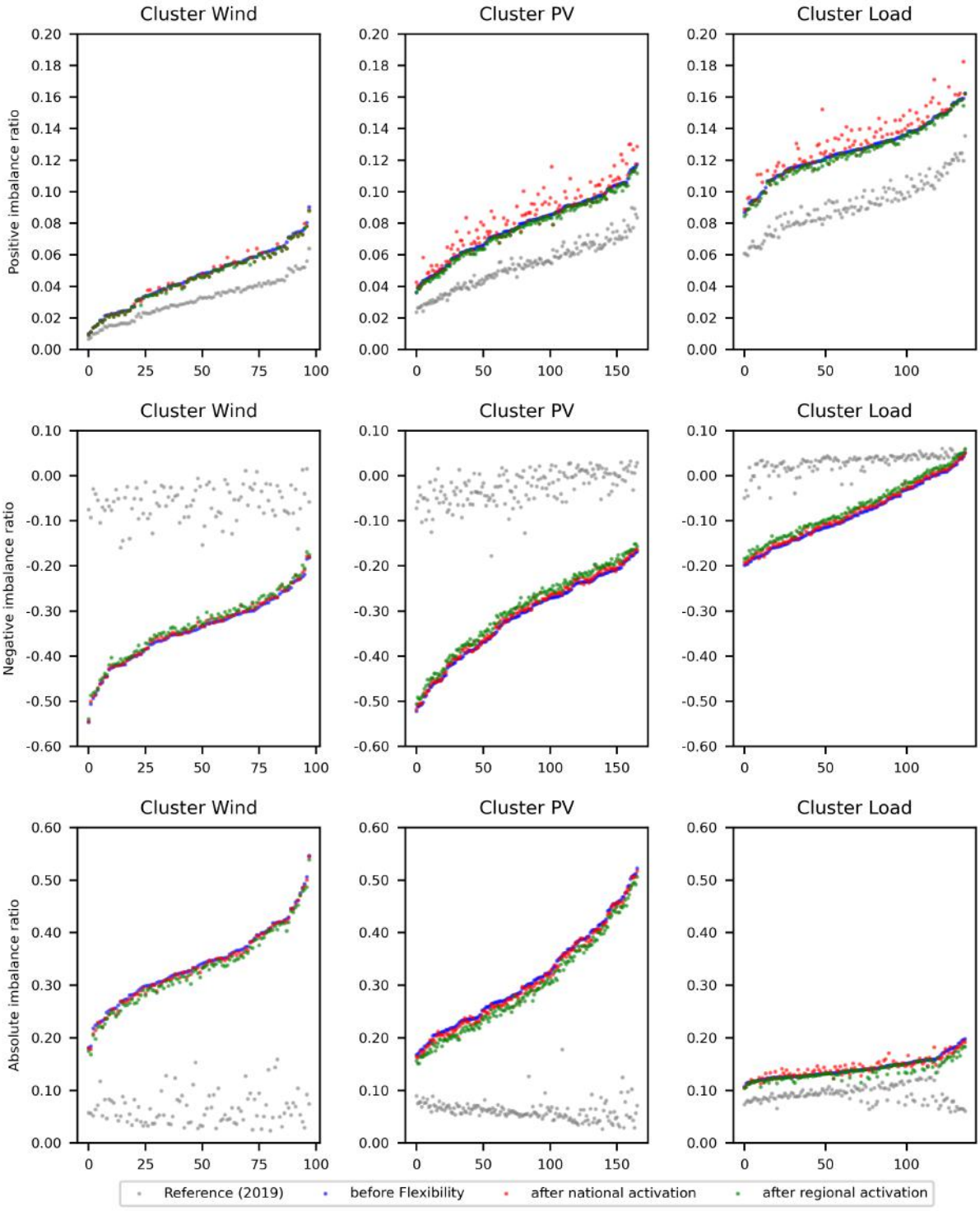

Figure 12: Imbalance ratios before and after the use of flexibility in 2045

Note: The x-axis represents the regions in each cluster. In each of the nine sub-figures, the imbalances before flexibility are sorted in ascending order. The imbalance ratios after the activation of flexibility are then matched to the corresponding region.

In renewable-dominated regions in 2045, before the activation of flexibility, the negative imbalance ratio is always greater, in absolute terms, than the positive imbalance ratio. It thus defines the absolute imbalance ratio and the maximum strain on local grid components. In the load-dominated cluster, it is the other way around in about 66% of the regions.

In the **Cluster Wind**, the positive imbalance ratio decreases only slightly when applying both activation mechanisms for flexibility. On average, positive imbalance declines by 1.2% with national incentives and by 2.7% with regional ones. The positive peaks of the residual loads decrease by 0.002 MW/km^2 on average with national incentives and by 0.004 MW/km^2 with the regional approach. The decreasing effect is limited by low positive flexibility potentials and the fact that the charging processes and the situation of the highest residual load do not fall into the same periods, as discussed in Section 5.1. The correlation between residual load and charging profile decreases over time, which limits the potential for flexibility in peak load situations. This limitation applies to all three clusters. The negative imbalance ratio in the wind-dominated cluster remains largely unchanged under the national deployment strategy (-1.2% on average in absolute terms[9], corresponding to -0.013 MW/km^2). However, it decreases more when applying the regional strategy (-3.5% in absolute terms, corresponding to -0.037 MW/km^2). As the negative imbalance ratio is greater than the positive one for the regions in this cluster, the absolute imbalance ratio reproduces the negative one in absolute terms.

In the **Cluster PV**, the positive imbalance ratios display a different pattern than the ones in the wind-dominated cluster, with an increase in response to national incentives. The national deployment strategy results in an increase of 5.1% of the positive imbalance ratio on average, which corresponds to an increase of the positive residual peak demand of 0.008 MW/km^2 across all regions within this cluster. But, there are also regions which face distinct greater effects with up to 0.071 MW/km^2. In these cases, peaks can increase by up to 35% following national incentives. This outcome is attributed to more electric vehicles in PV-dominated regions, resulting in a greater potential for positive flexibility. In contrast, positive imbalance ratios are lowered by 2.1% with

[9]For the positive and absolute imbalance ratio, a reduction corresponds to an improvement: the (positive or negative) residual load peak becomes smaller. For the negative imbalance ratio, a reduction corresponds to a worsening: the negative residual load peaks (the absolute value) become larger. In order to be consistent in terms of the positive/negative impact, all described changes in the negative imbalance ratio refer to the absolute change.

regional incentives on average, corresponding to a reduction of 0.008 MW/km^2 . The negative imbalance ratio is consistently reduced by regional incentives in absolute terms (-6.3% on average, corresponding to -0.068 MW/km^2). National incentives reduce the absolute value of the negative imbalance ratio, too, but to a less extent (-1.2%; -0.023 MW/km^2). Just as in the wind-dominated cluster, as the negative imbalance ratio is greater than the positive one, the absolute imbalance ratio reproduces the negative one in absolute terms. Last, in the **load-dominated cluster**, we observe that following national incentivized activation of flexibility, positive imbalance ratios are the highest compared to their occurrence in renewable-dominated clusters. On average, the positive imbalance increases by 3.1% (0.043 MW/km^2) with national incentives. But, just like in the PV-dominated cluster, there are also regions with high penetration rates of electric vehicles, which face a distinct greater effect with up to 0.349 MW/km^2. In this case, the peak increases by around 27% following national incentives. Regional incentives instead lower the positive imbalance ratio by 1.4% (-0.018 MW/km^2) on average. The negative imbalance ratio is consistently reduced both by regional and national incentives, but regional incentives have a greater effect (-2.1% compared to -6.3%, corresponding to -0.079 MW/km^2 and -0.208 MW/km^2). In contrast to the separated effects on positive and negative imbalances, the effect of national incentives on the absolute imbalance ratio is region-specific, indicating the regions' heterogeneity in the load-dominated cluster. In some regions, the positive imbalance ratio exceeds the negative imbalance ratio (regions 0 to 90), while the opposite is true in others (regions 91 to 137). In regions with a greater positive imbalance than a negative, the absolute imbalance ratio increases by 3.2% on average with national incentives, corresponding to an increase of absolute residual peak demand by 0.056 MW/km^2 on average. Instead, local incentives lower the absolute imbalance ratio by 1.1% on average, corresponding to a decrease of the absolute peak by 0.019 MW/km^2 on average. In regions with a smaller positive imbalance than a negative, national incentives reduce the absolute imbalance ration by 1.9% on average (-0.036 MW/km^2), whereas local incentives would lower the absolute imbalance ratio even more by 5.9% (-0.104 MW/km^2) on average. Consequently, there are regions in the load-dominated cluster where national incentives are slightly beneficial in lowering the absolute imbalance ratio or do not significantly change it. However, there are also regions where national incentives result in

an increase in the absolute imbalance ratio, stemming from the increase in positive peaks. Or, formulated differently, national incentives can significantly increase or slightly reduce the absolute peaks. Regional incentives may either lower the imbalance ratio or have an insignificant impact on the absolute value, depending on the flexibility potential and the correlation between charging profiles and residual load peaks.

Summarizing, national incentives tend to increase the positive imbalance ratio in PV- and load-dominated regions, whereas regional incentives decrease it, albeit to a small extent. However, regional incentives can significantly reduce the negative imbalance ratio.
In the context of the three clusters under consideration, it can be inferred that in regions dominated by wind energy, the national deployment strategy does not exert additional pressure on the distribution grid, but regional incentives can reduce imbalances. In PV-dominated regions, both the national and the regional incentives do lower the absolute imbalance ratio. However, regional incentives have a greater effect. For the regions of both clusters, it can be observed that the flexibility potential is used in particular to absorb excess renewable electricity and has less effect in smoothing load peaks. This is also manifested in the temporal shift patterns in the two clusters: For both the national and the regional incentivization, load shifting takes place primarily from the evening to the times of surplus generation at noon.
In contrast, load-dominated regions are characterized by heterogeneity in terms of positive or negative peak dominance, so the impact of national incentives on imbalances can be either positive (worsen the situation) or negligible. That is because the national incentivization corresponds to the temporal scheme of the renewable-dominated regions: Load is shifted from the evening into the times of national renewable surplus, only that there is no renewable energy surplus in many load-dominated regions, leaving them worse off. Regional incentives, on the other hand, can reduce absolute imbalances in these regions, as the load is shifted into the night, to address load peaks during the day.

6. Conclusion

The expansion of decentralized renewable energy systems and electric vehicles is putting stress on the distribution grids. However, flexible EV charging can help alleviate this impact by reducing peak loads and feed-in by better matching load and supply. The paper conducted a comprehensive regional analysis of Germany to estimate the regional potential of EV charging flexibility for reducing peaks on regional and national levels. This was achieved by modeling regional EV diffusion with sigmoid functions and deriving individual charging and flexibility profiles for each NUTS 3 region in Germany. For both, we presented a detailed method. We further developed a model to optimize the use of EV charging flexibility to either flatten the regional residual loads or the national one.
Our analysis consists of two parts.
In the first part of our analysis, we examined the future development of residual load curves and their correlation with EV charging profiles. Three different clusters were formed: load-dominated, wind-dominated and PV-dominated. We find that the increased dependency on weather-based electricity generation leads to a significant increase in the variance of the residual load curve until 2045. Our results reveal that the regional structure of electricity demand and supply is highly heterogeneous. Moreover, the correlation between residual load and EV charging profiles decreases over time, implying that the marginal utility of charging flexibility to reduce load peaks declines, even if the positive flexibility potential increases in absolute terms.
In the second part, we evaluated the impact of two incentive mechanisms for activating the flexibility of electric vehicles. One aims to flatten the regional residual load curves with local flexibility. The other uses the aggregated flexibility potentials to flatten the national residual load. Results show that both strategies reduce the variance of the residual load and peak demand and feed-in from a national perspective. In 2045, both strategies reduce the positive residual peak load by about 4 GW (3.6%), correspondingly less reserve capacity, storage or imports need to be kept available. The negative residual peak load, i.e. the maximum surplus of renewable capacity, is reduced by 15 GW (5.0%) in case of regional incentivization and even by 18 GW (5.9%) in case of national incentivization. I.e., the use of EV charging flexibility has a significantly greater potential in absorbing excess renewable generation than in lowering positive peak load. Regional incentivization generally

leads to a decline in absolute values of peaks on regional level. Here, as well, the flexibility is particularly useful in absorbing excess renewable generation and thus reducing negative residual load peaks. The local impact of the national incentivized activation varies depending on the region's characteristics. In load- and some PV-dominated regions, national incentivization can result in drastically higher regional demand peaks compared to a scenario without charging flexibility (up to 35%). In wind-dominated regions, this effect is less pronounced. Furthermore, regions with higher shares of EV load than total load and regions with a higher correlation of EV charging profiles with the residual load have higher potential to flatten the residual load and reduce the peak demand.

The two application scenarios of charging flexibility discussed aim at two very different targets: while national incentivization aims at reducing demand in times of low national renewable generation feed-in and thus times of high prices, the regional incentivization aims at reducing the regional strain on grid components. Our study shows that these two targets can be contradictory in their effects: While the regional incentivization is less effective in reaching the smoothing in the national residual demand curve, the national incentivization can even lead to increased strain on local level, especially in load-dominated regions. Policymakers should, thus, consider these regional effects when implementing incentives for flexible EV charging to achieve maximum effectiveness in reducing peaks on regional and/or national levels and avoid unwanted, additional strain on grid components. Furthermore, our results may also provide a justification at the transmission system level for introducing regionally differentiated price signals (e.g. zonal or nodal pricing), as uniform pricing at the national level may result in undesirable effects at the regional level.

While we are able to estimate regional effects of flexibility deployment at the level of NUTS 3 regions with our method, there is a need for further research on its impact on actual distribution grids and grid components. In the course of this, the concrete grid expansion costs and electricity generation costs under different deployment strategies could be quantified and compared. Furthermore, our analysis abstracts from other flexibility options and their interdependencies with the flexible home charging of EVs. Hence, there remains a need for further research, addressing workplace charging or charging in public spaces as well. Finally, further research could investigate on the effects of different policy schemes aiming at the implementation of the discussed deployment strategies.

Acknowledgements

The authors would like to thank Marc Oliver Bettzüge, Matti Liski, Philipp Theile, Jonas Zinke and Philip Horster for thoughtful and constructive comments and discussions on this work.

Funding: This work was supported by the German Federal Ministry of Education and Research (BMBF) within the Kopernikus-project 'New ENergy grid StructURes for the German Energiewende' (ENSURE) (grant number 03SFK1L0-2), as well as the German Federal Ministery of Economy and Climate protection within the project 'GreenVEgaS - Gesamtsystemanalyse der Sektorenkopplung – Volkswirtschaftliche Bewertung der Energieinfrastruktur und –erzeugung für eine Kopplung der Sektoren Strom, Wärme und Verkehr' (grant number 03EI1009C).

References

Agora Verkehrswende, Agora Energiewende and Regulatory Assistance Project (RAP) (2019). Verteilnetzausbau für die Energiewende – Elektromobilität im Fokus. https://static.agora-energiewende.de/fileadmin/Projekte/2018/Netzausbau_Elektromobilitaet/AgoraRAP2019_VerteilnetzausbauElektromobilitaet.pdf, accessed: 02.03.2023.

Amann, G., Bermúdez, V., Kovacs, E. B., Gallego, S., Giannelos, S., Iliceto, A. et al. (2022). E-Mobility Deployment and Impact on Grids: Impact of EV and Charging Infrastructure on European T&D Grids - Innovation Needs. https://smart-networks-energy-transition.ec.europa.eu/system/files/2022-12/ETIP%20SNET%20E-Mobility%20White%20Paper_pdf.pdf, accessed: 02.03.2023.

Ayyadi, S. and Maaroufi, M. (2018). Diffusion Models For Predicting Electric Vehicles Market in Morocco. In *2018 International Conference and Exposition on Electrical And Power Engineering (EPE)*, 0046–0051, doi:10.1109/ICEPE.2018.8559858.

Bass, F. M. (1969). A new product growth for model consumer durables. *Management Science* 15: 215–227.

BBSR (2022). Laufende Raumbeobachtung - Raumabgrenzungen: Siedlungsstrukturelle Gebietstypen. https://www.bbsr.bund.de/BBSR/DE/forschung/raumbeobachtung/Raumabgrenzungen/deutschland/kreisgebietsreformen/SiedlungsstrukturelleGebietstypen_alt/gebietstypen.html.

Becker, T. A., Sidhu, I. and Tenderich, B. (2009). Electric vehicles in the US a new model with forecasts to 2030. *Center for Entrepreneuship and technology, University of California, Berkeley* 2009.1.v.2.0, https://www.globaltrends.thedialogue.org/wp-content/uploads/2014/12/Electric-Vehicles-in-the-United-States-A-New-Model-with-Forecasts-to-2030.pdf, accessed: 02.03.2023.

Berger, R. (1981). Comparison of the Gompertz and Logistic Equations to Describe Plant Disease Progress. *Phytopathology* 71: 716–719, https://www.apsnet.org/publications/phytopathology/backissues/Documents/1981Articles/Phyto71n07_716.PDF, accessed: 02.03.2023.

BNetzA (2020). Bundesnetzagentur für Elektrizität, Gas, Telekommunikation, Post und Eisenbahnen - Genehmigung des Szenariorahmens 2021-2035. https://www.netzentwicklungsplan.de/sites/default/files/paragraphs-files/Szenariorahmen_2035_Genehmigung_1.pdf.

BNetzA (2022). Markstammdatenregister. https://www.marktstammdatenregister.de/MaStR.

Bundesrat (2022). Gesetz zu Sofortmaßnahmen für einen beschleunigten Ausbau der erneuerbaren Energien und weiteren Maßnahmen im Stromsektor. https://www.clearingstelle-eeg-kwkg.de/sites/default/files/2022-07/0315-22.pdf.

Burchardt, J., Franke, K., Herhold, P., Hohaus, M., Humpert, H., Päivärinta, J., Richenhagen, E., Ritter, D., Schönberger, S., Schröder, J. et al. (2021). Klimapfade 2.0– Ein Wirtschaftsprogramm für Klima und Zukunft. https://web-assets.bcg.com/f2/de/1fd134914bfaa34c51e07718709b/klimapfade2-gesamtstudie-vorabversion-de.pdf.

CEER, Council of European Energy Regulators (2020). CEER Paper on DSO Procedures of Procurement of Flexibility. https://www.ceer.eu/documents/104400/-/-/f65ef568-dd7b-4f8c-d182-b04fc1656e58.

Consentec, Fraunhofer ISI, TU Berlin and ifeu (2021). Langfristszenarien für die Transformation des Energiesystems in Deutschland 3. https://www.isi.fraunhofer.de/content/dam/isi/dokumente/cce/2021/LFS_Kurzbericht.pdf.

Copernicus Climate Change Service (2020). Climate and energy indicators for Europe from 1979 to present derived from reanalysis. Copernicus Climate Change Service (C3S) Climate Data Store (CDS). (Accessed 06-02-2023). doi:10.24381/cds.4bd77450.

Council of European Union and European Parliament (2019). Directive (EU) 2019/944 of the European Parliament and of the Council. http:https://eur-lex.europa.eu/legal-content/EN/TXT/PDF/?uri=CELEX:32019L0944&from=EN.

dena (2018). dena-Leitstudie integrierte Energiewende: Impulse für die gestaltung des energiesystems bis 2050. Deutsche Energie-Agentur GmbH (dena), ewi Energy Research & Scenarios gGmbH: Berlin/Köln, Germany. https://www.dena.de/fileadmin/dena/Dokumente/Pdf/9262_dena-Leitstudie_Integrierte_Energiewende_Ergebnisbericht.pdf.

dena (2021). dena Leitstudie - Aufbruch Klimaneutralität. https://www.dena.de/fileadmin/dena/Publikationen/PDFs/2021/Alle_Gutachten_dena-Leitsudie_Aufbruch_Klimaneutralitaet.pdf.

dena (2022). Vergleich der „Big 5"-Klimaneutralitätsszenarien. https://www.dena.de/newsroom/publikationsdetailansicht/pub/vergleich-der-big-5-klimaneutralitaetsszenarien/.

dena and Prognos (2020). Privates Ladeinfrastrukturpotenzial in Deutschland. https://www.dena.de/fileadmin/dena/Publikationen/PDFs/2020/dena-STUDIE_Privates_Ladeinfrastrukturpotenzial_in_Deutschland.pdf.

Deutscher Bundestag (2021). Erstes Gesetz zur Änderung des Bundes-Klimaschutzgesetzes, Bundesgesetzblatt Jahrgang 2021 Teil I Nr. 59, ausgegeben zu Bonn am 30. August 2021. https://www.bgbl.de/xaver/bgbl/start.xav?startbk=Bundesanzeiger_BGBl&start=//*%5B@attr_id=%27bgbl121s3905.pdf%27%5D#__bgbl__%2F%2F*%5B%40attr_id%3D%27bgbl121s3905.pdf%27%5D__1675782713390.

Ebner, M., Fiedler, C., Jetter, F. and Schmid, T. (2019). Regionalized Potential Assessment of Variable Renewable Energy Sources in Europe. In *2019 16th International Conference on the*

European Energy Market (EEM), 1–5, doi:10.1109/EEM.2019.8916317.

ENTSO-E (2022a). Actual Generation per Production Type. https://transparency.entsoe.eu/generation/r2/actualGenerationPerProductionType/show.

ENTSO-E (2022b). National estimates scenario ERAA 2021 - Hourly demand time-series, Demand Forecasting Methodology. https://eepublicdownloads.azureedge.net/clean-documents/sdc-documents/ERAA/Demand%20Forecasting%20Methodology%20and%20Insights%20(ERAA%202021).pdf.

Flataker, A., Malmin, O. K., Hjelkrem, O. A., Rana, R., Korpås, M. and Torsæter, B. N. (2022). Impact of home- and destination charging on the geographical and temporal distribution of electric vehicle charging load. In *2022 18th International Conference on the European Energy Market (EEM)*, 1–6, doi:10.1109/EEM54602.2022.9921062.

German Government (2022). Nachhaltige Mobilität - Nicht weniger fortbewegen, sondern anders. https://www.bundesregierung.de/breg-de/themen/klimaschutz/nachhaltige-mobilitaet-2044132#:~:text=Nachhaltige%20Mobilit%C3%A4t%20Nicht%20weniger%20fortbewegen,um%20%C3%BCber%2040%20Prozent%20sinken.

German TSOs (2022). Szenariorahmen zum Netzentwicklungsplan Strom 2037 mit Ausblick 2045, Version 2023, Entwurf der Übertragungsnetzbetreiber. https://www.netzentwicklungsplan.de/sites/default/files/paragraphs-files/Szenariorahmenentwurf_NEP2037_2023.pdf.

Gompertz, B. (1825). Xxiv. on the nature of the function expressive of the law of human mortality, and on a new mode of determining the value of life contingencies. in a letter to francis baily, esq. frs &c. *Philosophical transactions of the Royal Society of London* : 513–583.

Gunkel, P. A., Bergaentzlé, C., Græsted Jensen, I. and Scheller, F. (2020). From passive to active: Flexibility from electric vehicles in the context of transmission system development. *Applied Energy* 277: 115526, doi:https://doi.org/10.1016/j.apenergy.2020.115526.

HErZ, Hans-Ertel Centre for Weather Research (University of Bonn - Germany) and DWD, Deutscher Wetterdienst (2022). COSMO-REA6. https://reanalysis.meteo.uni-bonn.de/?Download_Data___COSMO-REA6.

Huld, T., Gottschalg, R., Beyer, H. G. and Topič, M. (2010). Mapping the performance of PV modules, effects of module type and data averaging. *Solar Energy* 84: 324–338, doi:https://doi.org/10.1016/j.solener.2009.12.002.

infas, DLR, IVT and infas 360 (2018). Mobilität in Deutschland (im Auftrag des BMVI). www.mobilitaet-in-deutschland.de.

KIT - Institut für Verkehrswesen (2021). Deutsches Mobilitätspanel (MOP) – Wissenschaftliche Begleitung und Auswertungen Bericht 2020/2021: Alltagsmobilität und Fahrleistung. https:

//mobilitaetspanel.ifv.kit.edu/downloads/Bericht_MOP_20_21.pdf.

Kockel, C., Nolting, L., Priesmann, J. and Praktiknjo, A. (2022). Does renewable electricity supply match with energy demand? A spatio-temporal analysis for the German case. *Applied Energy* 308: 118226, doi:https://doi.org/10.1016/j.apenergy.2021.118226.

Kopernikus-Projekt Ariadne (2021). Ariadne-Report: Deutschland auf dem Weg zur Klimaneutralität 2045 - Szenarien und Pfade im Modellvergleich. doi:0.48485/pik.2021.006.

Kraftfahrt-Bundesamt (2018a). Bestand an Kraftfahrzeugen und Kraftfahrzeuganhängern nach Gemeinden, 1. Januar 2018 (FZ 3). https://www.kba.de/DE/Statistik/Produktkatalog/produkte/Fahrzeuge/fz3_b_uebersicht.html?nn=3514348.

Kraftfahrt-Bundesamt (2018b). Bestand an Kraftfahrzeugen und Kraftfahrzeuganhängern nach Zulassungsbezirken, 1. Januar 2018 (FZ 1). https://www.kba.de/DE/Statistik/Produktkatalog/produkte/Fahrzeuge/fz1_b_uebersicht.html?nn=3514348.

Kraftfahrt-Bundesamt (2019a). Bestand an Kraftfahrzeugen und Kraftfahrzeuganhängern nach Gemeinden, 1. Januar 2019 (FZ 3). https://www.kba.de/DE/Statistik/Produktkatalog/produkte/Fahrzeuge/fz3_b_uebersicht.html?nn=3514348.

Kraftfahrt-Bundesamt (2019b). Bestand an Kraftfahrzeugen und Kraftfahrzeuganhängern nach Zulassungsbezirken, 1. Januar 2019 (FZ 1). https://www.kba.de/DE/Statistik/Produktkatalog/produkte/Fahrzeuge/fz1_b_uebersicht.html?nn=3514348.

Kraftfahrt-Bundesamt (2020a). Bestand an Kraftfahrzeugen und Kraftfahrzeuganhängern nach Gemeinden, 1. Januar 2020 (FZ 3). https://www.kba.de/DE/Statistik/Produktkatalog/produkte/Fahrzeuge/fz3_b_uebersicht.html?nn=3514348.

Kraftfahrt-Bundesamt (2020b). Bestand an Kraftfahrzeugen und Kraftfahrzeuganhängern nach Zulassungsbezirken, 1. Januar 2020 (FZ 1). https://www.kba.de/DE/Statistik/Produktkatalog/produkte/Fahrzeuge/fz1_b_uebersicht.html?nn=3514348.

Kraftfahrt-Bundesamt (2021a). Bestand an Kraftfahrzeugen und Kraftfahrzeuganhängern nach Gemeinden, 1. Januar 2021 (FZ 3). https://www.kba.de/DE/Statistik/Produktkatalog/produkte/Fahrzeuge/fz3_b_uebersicht.html?nn=3514348.

Kraftfahrt-Bundesamt (2021b). Bestand an Kraftfahrzeugen und Kraftfahrzeuganhängern nach Zulassungsbezirken, 1. Januar 2021 (FZ 1). https://www.kba.de/DE/Statistik/Produktkatalog/produkte/Fahrzeuge/fz1_b_uebersicht.html?nn=3514348.

Kumar, R. R., Guha, P. and Chakraborty, A. (2022). Comparative assessment and selection of electric vehicle diffusion models: A global outlook. *Energy* 238: 121932, doi:https://doi.org/10.1016/j.energy.2021.121932.

Kühnbach, M., Bekk, A. and Weidlich, A. (2021). Prepared for regional self-supply? On the regional fit of electricity demand and supply in Germany. *Energy Strategy Reviews* 34: 100609, doi: https://doi.org/10.1016/j.esr.2020.100609.

Länderarbeitskreis Energiebilanzen (2022). Vollständige Energiebilanz. https://www.lak-energiebilanzen.de/eingabe-dynamisch/?a=e900, accessed: 2022-11-03.

Muraleedharakurup, G., McGordon, A., Poxon, J. and Jennings, P. (2010). Building a better business case: the use of non-linear growth models for predicting the market for hybrid vehicles in the uk. *Ecological Vehicles and Renewable Energies. Monaco* .

Newville, M., Stensitzki, T., Allen, D. B., Rawlik, M., Ingargiola, A. and Nelson, A. (2016). Lmfit: Non-Linear Least-Square Minimization and Curve-Fitting for Python. Astrophysics Source Code Library, record ascl:1606.014.

Pavlidou, A. (2010). Diffusion of the diffusion curve: A research on the SS-curvescurves in relation to technological clusters. *Utrecht University, Faculuty of Geoscience, Utrecht* .

Powell, S., Cezar, G. V., Min, L., Azevedo, I. M. L. and Rajagopal, R. (2022). Charging infrastructure access and operation to reduce the grid impacts of deep electric vehicle adoption. *Nature Energy* 7: 932–945, doi:10.1038/s41560-022-01105-7.

Prognos, Öko-Institut and Wuppertal-Institut (2020). Klimaneutrales Deutschland. Studie im Auftrag von Agora Energiewende, Agora Verkehrswende und Stiftung Klimaneutralität. https://static.agora-energiewende.de/fileadmin/Projekte/2021/2021_04_KNDE45/A-EW_209_KNDE2045_Zusammenfassung_DE_WEB.pdf.

Radecke, J., Hefele, J. and Hirth, L. (2019). Markets for Local Flexibility in Distribution Networks A Review of European Proposals for Market-based Congestion Management in Smart Grids. *ZBW – Leibniz Information Centre for Economics, Kiel, Hamburg* .

Rebenaque, O., Schmitt, C., Schumann, K., Dronne, T. and Roques, F. (2023). Success of local flexibility market implementation: A review of current projects. *Utilities Policy* 80: 101491, doi:https://doi.org/10.1016/j.jup.2023.101491.

Ruhnau, O. and Muessel, J. (2022). When2heat heating profiles. open power system data. doi: https://doi.org/10.25832/when2heat/2022-02-22.

Song, X. (2013). Forecast of electric vehicles in china based on bass model. *Electric Power* .

SWM (2022). Lastprofil Wärmepumpe. https://www.swm-infrastruktur.de/strom/netzzugang/bedingungen/waermepumpe.

Van der Kam, M., Meelen, A., van Sark, W. and Alkemade, F. (2018). Diffusion of solar photovoltaic systems and electric vehicles among dutch consumers: Implications for the energy transition. *Energy Research & Social Science* 46: 68–85, doi:https://doi.org/10.1016/j.erss.2018.06.003.

VDEW (1999). Repräsentative VDEW-Lastprofile. https://www.bdew.de/energie/standardlastprofile-strom/.

VWG (2022a) (2022). Bruttoinlandsprodukt, bruttowertschöpfung in den kreisfreien städten und landkreisen der bundesrepublik deutschland 1992 und 1994 bis 2020, reihe 2, kreisergebnisse band 1, berechnungsstand: November 2021.

VWG (2022b) (2022). Arbeitnehmerentgelt, bruttolöhne und -gehälter in den kreisfreien städten und landkreisen der bundesrepublik deutschland 2000 bis 2020, reihe 2, kreisergebnisse band 2, berechnungsstand: November 2021.

Won, J.-R., Yoon, Y.-B. and Lee, K.-J. (2009). Prediction of electricity demand due to PHEVs(Plug-In Hybrid Electric Vehicles) distribution in Korea by using diffusion model. In *2009 Transmission & Distribution Conference & Exposition: Asia and Pacific*, 1–4, doi:10.1109/TD-ASIA.2009.5356888.

Zhu, Y., Tokimatsu, K. and Matsumoto, M. (2017). *Study on the Diffusion of NGVs in Japan and Other Nations Using the Bass Model*. Singapore: Springer Singapore, chap. VI-7. 765–778, doi:10.1007/978-981-10-0471-1_52.

Appendices

*A. **The full Bass model***

For the computation of regional transition pathways of electric vehicles, the Bass diffusion model is used. In this section, it is explained how the formula in Equation (3) is derived. According to Rogers' concept of the diffusion of innovation (1962), $P(t)$ is "the probability that an initial purchase will be made at time t given that no purchase has yet been made" (Bass, 1969).

$$P(t) = \frac{f(t)}{1 - F(t)} = p + \frac{q}{m}A(t) = p + qF(t) \tag{A.1}$$

The parameter p is the coefficient of innovators meaning the probability of initial purchases at the start of the innovation and q is the coefficient of imitators, signalling the pressure they feel from the increasing number and m is the total market size. $f(t)$ is the likelihood of purchase at time t. $F(t)$ is the cumulative diffusion level at time t, further described in Equation (A.2). $A(t)$ expresses the cumulative number of adopters $a(t)$ in the interval $(0, t)$, presented in Equation (A.3) (Bass, 1969; Van der Kam et al., 2018).

$$F(t) = \frac{A(t)}{m} = \int_0^t f(t)dt \tag{A.2}$$

$$A(t) = \int_0^T a(t)dt = m\int_0^T f(t)dt = mF(t) \tag{A.3}$$

The cumulative number of adopters $a(t)$ itself can be calculated according to Equation (A.4)

$$a(t) = mf(t) = P(t)[m - A(t)] = [p + \frac{q\int_0^T a(t)dt}{m}][m - \int_0^T a(t)dt] \tag{A.4}$$

Also, $f(t)$ can be extended as:

$$f(t) = [p + qF(t)][1 - F(t)] = p + (q - p)F(t) - q[F(t)]^2 \tag{A.5}$$

To find $F(t)$, this non-linear differential Equation (A.6) needs to be solved:

$$dt = \frac{dF}{(p + (q - p)F - qF)} \tag{A.6}$$

This equals to:

$$F = \frac{q - pe^{(-t+C)(p+q)}}{q(1 + e^{(-t+C)(p+q)})} \tag{A.7}$$

Since $F(0) = 0$, the integration constant may be evaluated:

$$-C = \frac{1}{p+q} ln(\frac{q}{p}) \tag{A.8}$$

Therefore:

$$F(t) = \frac{1 - e^{-(p+q)t}}{1 + \frac{q}{p}e^{-(p+q)t}} \tag{A.9}$$

or:

$$A(t) = m\frac{1 - e^{-(p+q)t}}{1 + \frac{q}{p}e^{-(p+q)t}} \tag{A.10}$$

To normalize the beginning of the diffusion t_0 at 0, this function can be written as:

$$A(t) = m\frac{1 - e^{-(p+q)(t-t_0)}}{1 + \frac{q}{p}e^{-(p+q)(t-t_0)}} \tag{A.11}$$

which is derived from Van der Kam et al. (2018).

B. *Function transformation to Δt*

This section displays the transformation of the diffusion curve function given in Equation (3) to the diffusion curve function in Equation (6). The objective is to calculate t given all other variables and parameters stay constant. Recall Equation (3):

$$F(t, \hat{m}, \hat{p}, \hat{q}) = \hat{m} * \frac{1 - e^{-(\hat{p}+\hat{q})(t-t_0)}}{1 + \frac{\hat{q}}{\hat{p}} e^{-(\hat{p}+\hat{q})(t-t_0)}} \qquad | * (1 + \frac{\hat{q}}{\hat{p}} e^{-(\hat{p}+\hat{q})(t-t_0)}) \tag{B.12}$$

For the sake of simplicity, $F(t)$ will be written as F in this function transformation. The transformation steps are shown in Equations (B.13) to (B.20).

$$F(1 + \frac{\hat{q}}{\hat{p}} e^{-(\hat{p}+\hat{q})(t-t_0)}) = \hat{m} * (1 - e^{-(\hat{p}+\hat{q})(t-t_0)}) \qquad |\text{solving the brackets} \tag{B.13}$$

$$F + F\frac{\hat{q}}{\hat{p}} e^{-(\hat{p}+\hat{q})(t-t_0)} = \hat{m} - \hat{m} e^{-(\hat{p}+\hat{q})(t-t_0)} \qquad | * \hat{p} \tag{B.14}$$

$$\hat{p}F + \hat{q}F e^{-(\hat{p}+\hat{q})(t-t_0)} = \hat{m}\hat{p} - \hat{m}\hat{p} e^{-(\hat{p}+\hat{q})(t-t_0)} \qquad | - \hat{p}F, + \hat{m}\hat{p} e^{-(\hat{p}+\hat{q})(t-t_0)} \tag{B.15}$$

$$\hat{m}\hat{p} e^{-(\hat{p}+\hat{q})(t-t_0)} + \hat{q}F e^{-(\hat{p}+\hat{q})(t-t_0)} = \hat{m}\hat{p} - \hat{p}F \tag{B.16}$$

$$(\hat{m}\hat{p} + \hat{q}F) e^{-(\hat{p}+\hat{q})(t-t_0)} = \hat{m}\hat{p} - \hat{p}F \qquad | * \frac{1}{\hat{m}\hat{p} + \hat{q}F} \tag{B.17}$$

$$e^{-(\hat{p}+\hat{q})(t-t_0)} = \frac{\hat{m}\hat{p} - \hat{q}F}{\hat{m}\hat{p} + \hat{q}F} \qquad |ln \tag{B.18}$$

$$-(\hat{p} + \hat{q})(t - t_0) = ln(\frac{\hat{m}\hat{p} - \hat{q}F}{\hat{m}\hat{p} + \hat{q}F}) \qquad | * \frac{1}{-(\hat{p} + \hat{q})} \tag{B.19}$$

$$t - t_0 = \frac{ln(\frac{\hat{m}\hat{p} - \hat{q}F}{\hat{m}\hat{p} + \hat{q}F})}{-(\hat{p} + \hat{q})} \qquad | + t_0 \tag{B.20}$$

$$t = \frac{ln(\frac{\hat{m}\hat{p} - \hat{q}F}{\hat{m}\hat{p} + \hat{q}F})}{-(\hat{p} + \hat{q})} + t_0 \tag{B.21}$$

To calculate the time difference Δt between a given time t_{set} when a NUTS 3 region reaches a certain diffusion level $F(t)_y^{nuts3}$, and the time when the same level is reached on the national diffusion curve, the following Equation (B.22) is the result.

$$\Delta t = t - t_{set} = t - \frac{ln(\frac{\hat{m}\hat{p} - \hat{q}F}{\hat{m}\hat{p} + \hat{q}F})}{-(\hat{p} + \hat{q})} + t_0 - t_{set} \tag{B.22}$$

C. *Descriptive analysis of mobility data*

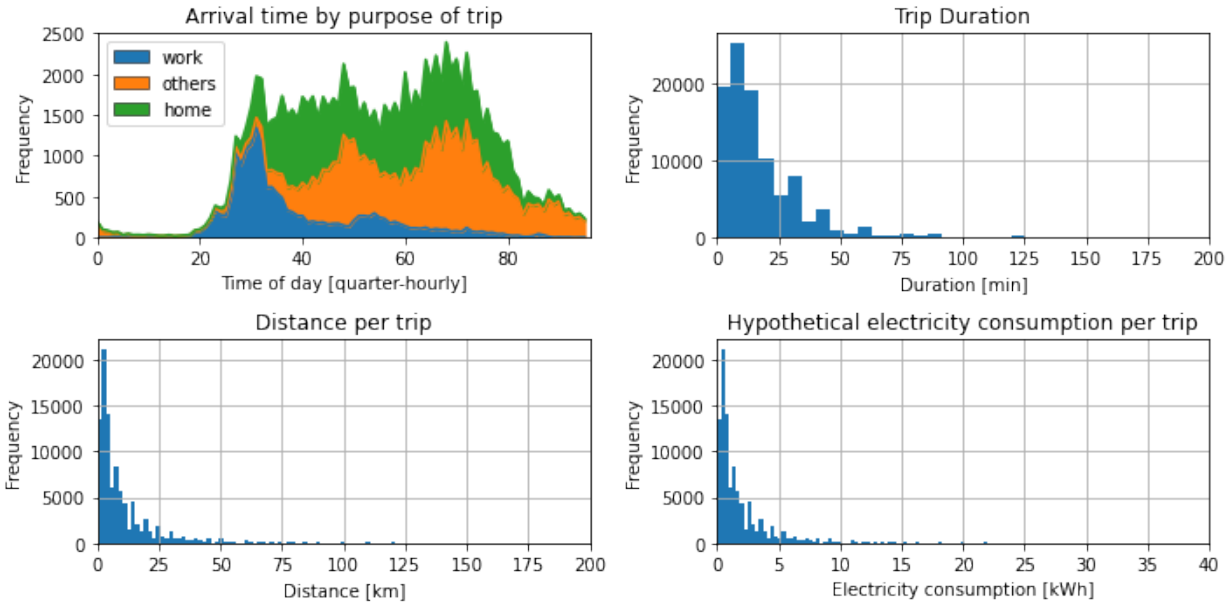

Figure C.1: Key parameters of the used MOP dataset (KIT - Institut für Verkehrswesen, 2021)

D. *Shares of charging scenarios*

Table D.1: Shares of charging scenarios per settlement type

settlement type	h	h,w	h,o	h,w,o	w	o	w,o	Total
rural community	22%	22%	22%	22%	4%	4%	4%	100%
smaller provincial town	22%	22%	22%	22%	4%	4%	4%	100%
larger provincial town	21%	21%	21%	21%	6%	6%	6%	100%
smaller medium town	18%	18%	18%	18%	9%	9%	9%	100%
larger medium town	20%	20%	20%	20%	7%	7%	7%	100%
smaller metropolis	16%	16%	16%	16%	13%	13%	13%	100%
larger metropolis	10%	10%	10%	10%	19%	19%	19%	100%

Notes: The row total may differ from 100% due to rounding errors. Charging locations: at home (h), at work (w), others (o)

*E. **Distribution of demand to federal states***

To distribute the national demand of each sector among the federal states, we use data from Länderarbeitskreis Energiebilanzen (2022). The data includes the demand of all federal states separately by sector for the years 1990-2019. We allocate the demand in our model among the federal states based on the distribution of sector-specific demand in 2019. An exception is the state of Saarland, where the most recent data available is from 2016 (Table E.2). We assume that this distribution does not change fundamentally over time.

Table E.2: Distribution keys of sectoral electricity demand to federal states

Sector	BW	BY	BE	BB	HB	HH	HE	MV	NI	NW	RP	SL	SN	ST	SH	TH	Total
Households	14%	16%	3%	3%	1%	3%	8%	2%	9%	23%	5%	1%	4%	2%	4%	2%	100%
Small-scale industries, trade and services	15%	16%	5%	3%	1%	3%	9%	2%	9%	20%	4%	1%	4%	3%	3%	3%	100%
Industry	12%	15%	1%	3%	1%	2%	5%	1%	11%	28%	7%	2%	5%	4%	2%	3%	100%
Rail transport	11%	19%	8%	5%	1%	3%	11%	2%	11%	15%	4%	1%	4%	4%	2%	2%	100%
Conversion sector	9%	9%	1%	10%	1%	3%	2%	1%	10%	37%	1%	2%	6%	5%	3%	0%	100%

Note: The row total may differ from 100% due to rounding errors.

*F. **Demand profiles***

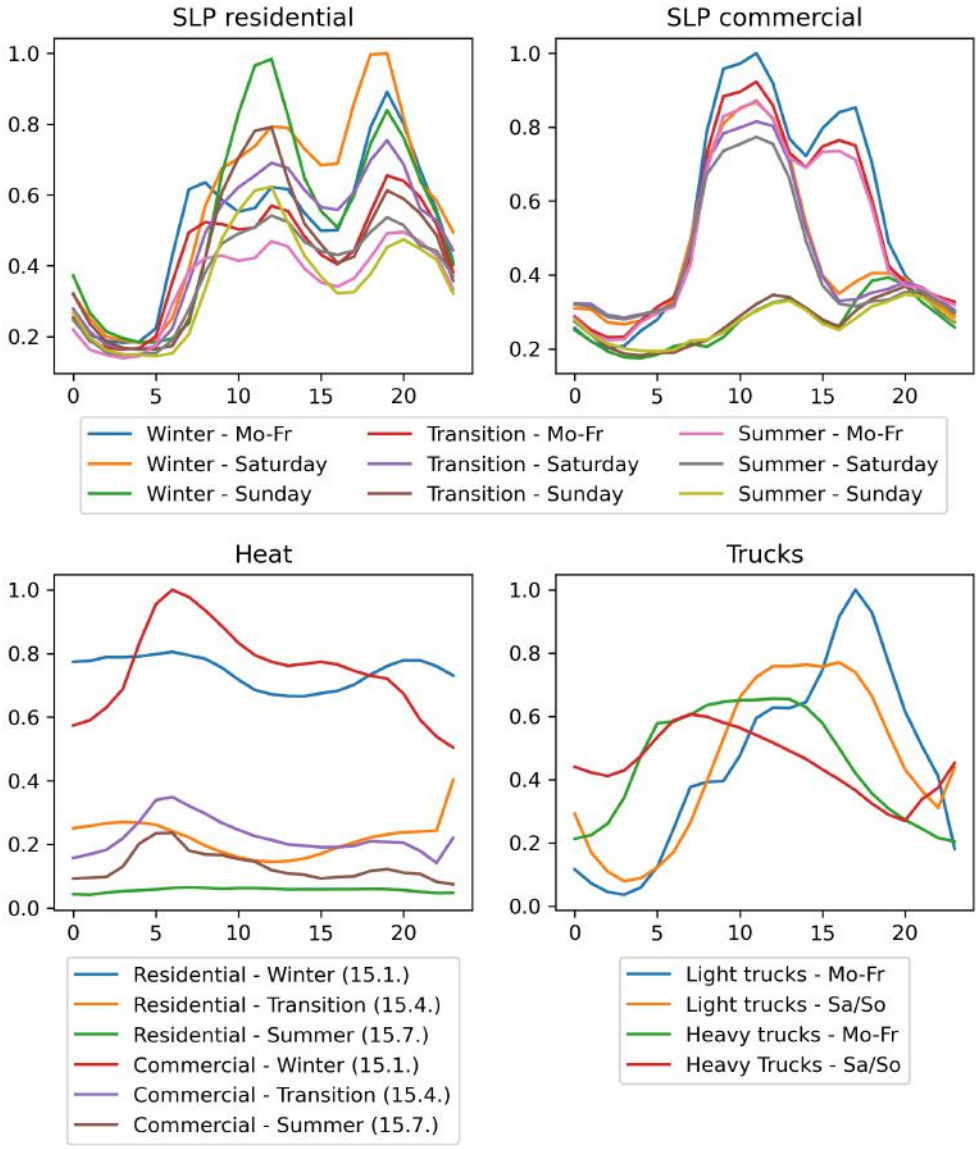

Figure F.2: Demand profiles per application. Heat profiles are exemplary: shown are the profiles for the region DEA23 (Cologne) on 3 exemplary days of the year.

G. *Cluster properties*

Table G.3: Properties of the regions within the three cluster in 2045

Property	Indicator	Cluster Wind	Cluster PV	Cluster Load
Population density	Minimum	36	66	125
[People per km^2]	Maximum	437	1585	4761
	Mean	117	264	1165
Number of EVs	Minimum	14	31	56
[cars per km^2]	Maximum	167	606	1811
	Mean	55	119	471
Wind Onshore capacity	Minimum	0.22	0.00	0.00
[MW per km^2]	Maximum	1.94	1.26	0.95
	Mean	0.75	0.29	0.15
total PV capacity	Minimum	0.19	0.16	0.00
[MW per km^2]	Maximum	1.59	2.18	2.35
	Mean	0.62	0.69	0.34
large-scale PV capacity	Minimum	0.19	0.16	0.00
[MW per km^2]	Maximum	1.59	2.18	2.34
	Mean	0.62	0.69	0.34
rooftop PV capacity	Minimum	0.13	0.15	0.23
[MW per km^2]	Maximum	2.04	5.41	7.46
	Mean	0.38	0.86	2.20

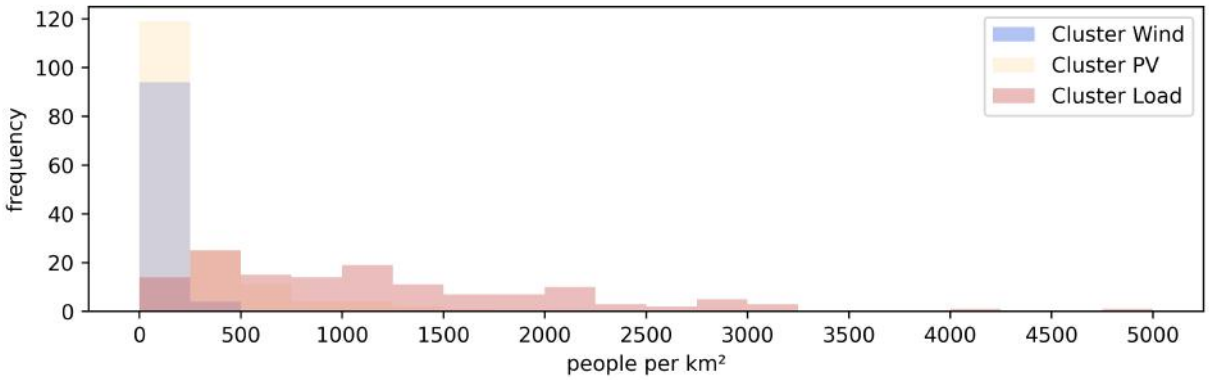

Figure G.3: Distribution of the population density within each cluster in 2045

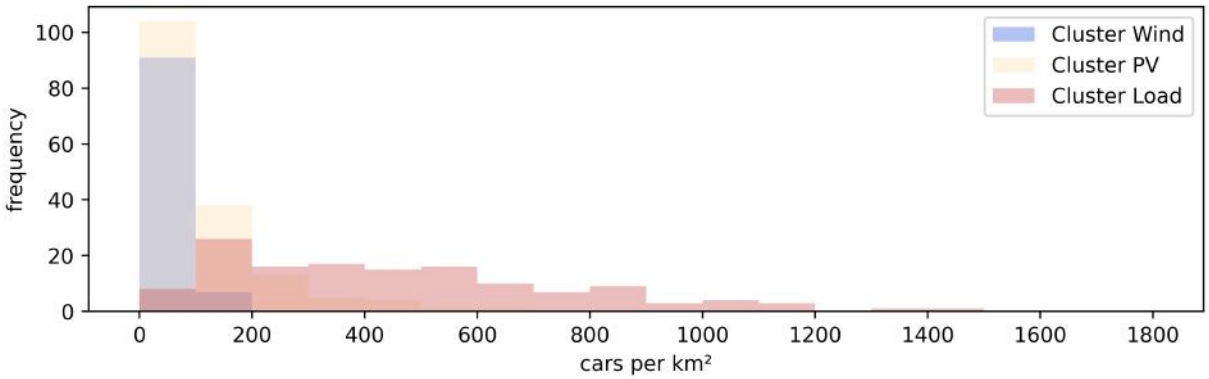

Figure G.4: Distribution of EVs per km^2 within each cluster in 2045

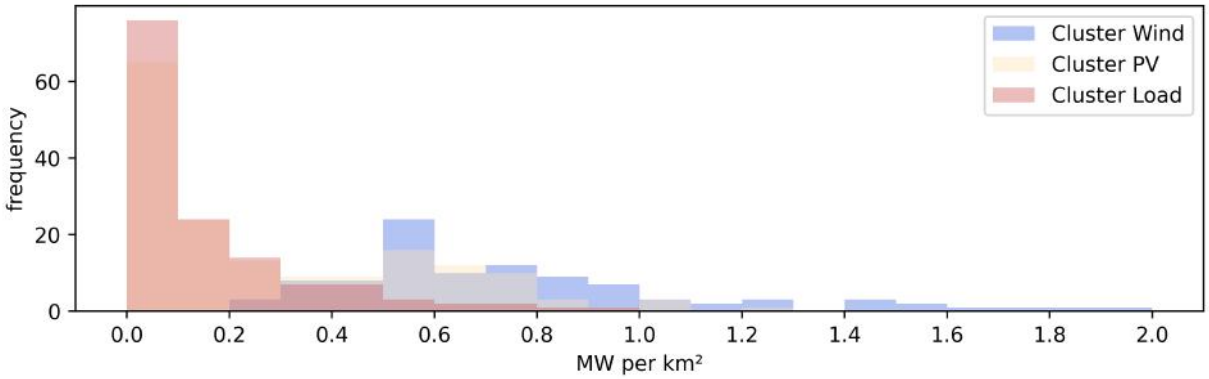

Figure G.5: Distribution of Wind Onshore capacities per km^2 within each cluster in 2045

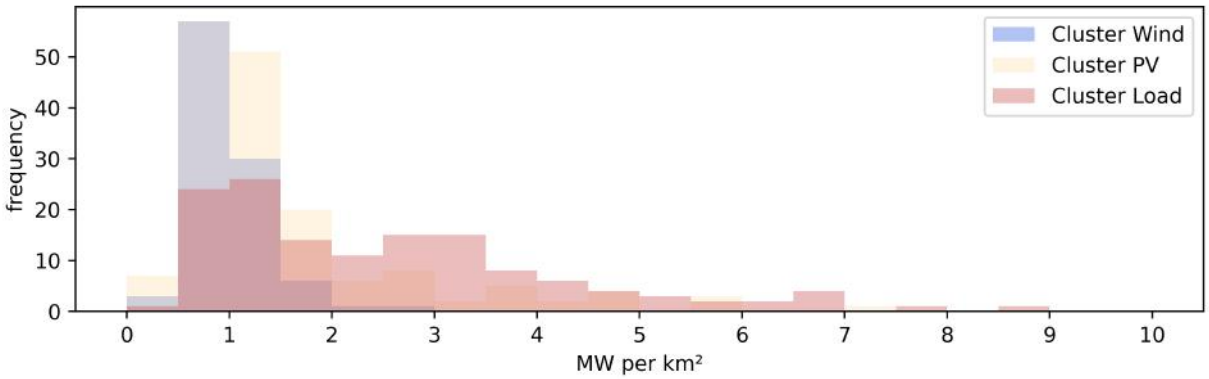

Figure G.6: Distribution of PV capacities (large-scale PV and rooftop PV) per km^2 within each cluster in 2045

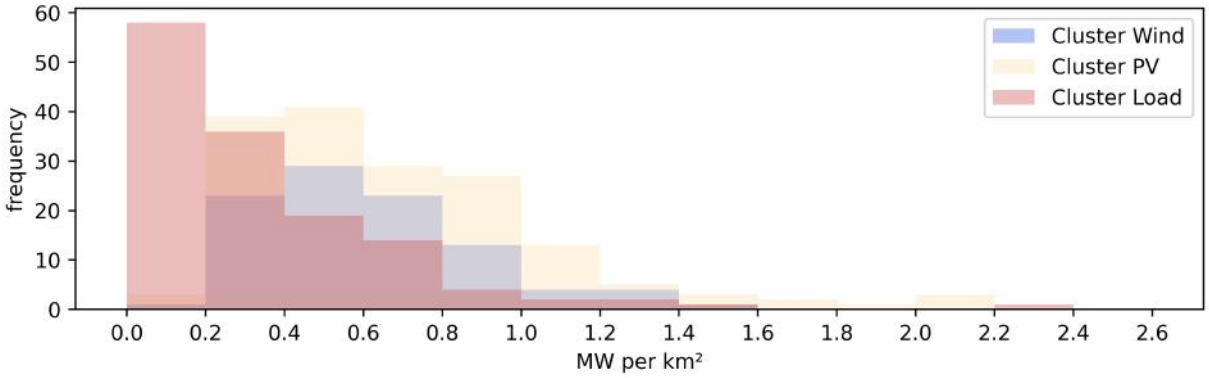

Figure G.7: Distribution of large-scale PV capacities per km^2 within each cluster in 2045

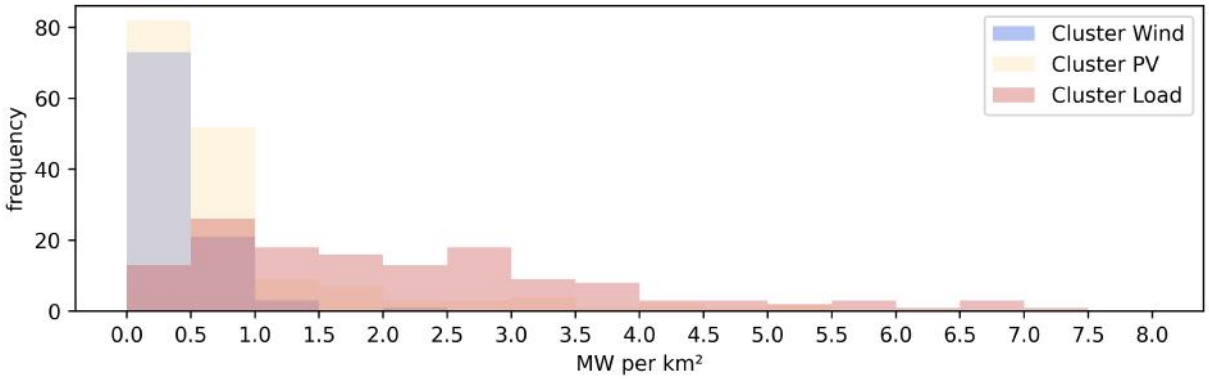

Figure G.8: Distribution of rooftop PV capacities per km^2 within each cluster in 2045